OPTIMIZATION OF AN AXIALLY COMPRESSED RING AND STRINGER STIFFENED CYLINDRICAL SHELL FOR SERVICE IN THE POST-LOCAL-BUCKLING REGIME AND EVALUATION OF THE OPTIMIZED SHELL WITH VARIOUS STAGS MODELS

David Bushnell

December 15, 2009

ABSTRACT

An elastic cylindrical shell with internal stringers and rings with rectangular cross sections is optimized with PANDA2. The material is isotropic (aluminum). The optimum design is developed under the condition that local buckling of the panel skin is permitted at a load much lower than the design load. In the optimized (minimum weight) design local buckling occurs at approximately one third of the design load. A small portion of the optimized design, a segment between two adjacent rings, is then analyzed with STAGS. In the STAGS models various boundary conditions are applied, and the STAGS predictions are compared with those from PANDA2. The best agreement between PANDA2 and STAGS is obtained for a STAGS model in which in-plane warping of the panel skin along the four panel edges is prevented, and overall axial bending of the panel in the post-local-buckling regime is prevented by forcing the axial displacement u to be uniform over the heights of the stringer webs at the two curved ends of the panel. Certain modifications of the PANDA2 processor, STAGSUNIT, which produces valid input files, *.bin and *.inp, for STAGS, were required in order to obtain the results presented here. These modifications are described. The agreement between STAGS and PANDA2 is much better than that obtained previously before the modifications to STAGSUNIT were implemented. It is emphasized that modifications to STAGSUNIT do not affect results obtained from PANDA2. PANDA2 and STAGS predictions are obtained for both curved and flat panels. STAGS predicts a higher, more concentrated local post-buckling maximum effective stress at the design load than does PANDA2, especially for STAGS models in which the panel curvature is included. The maximum effective stress concentration occurs in the panel skin adjacent to the root of each stringer. If the panel curvature is included in the STAGS model, STAGS predicts a maximum effective local post-buckling stress in the skin surface opposite from that to which the internal stringer is attached that is about 30% higher than that predicted by PANDA2. The maximum effective stress is about 20 per cent greater in the skin surface opposite from that where the stringers are attached than in the skin surface to which the stringers are attached. When the panel curvature is neglected in the STAGS model, STAGS predicts a maximum local post-buckling effective stress that is about 9% higher than that predicted by PANDA2, and the maximum effective stress is about the same on either surface of the panel skin. The difference between STAGS and PANDA2 results with regard to the local concentration of effective stress in the immediate neighborhood of each stringer web root is caused primarily by STAGS predicting a significantly higher and more localized concentration of post-buckling change in circumferential curvature at the design load than does PANDA2, especially for the curved panels. Local post-buckling deformations and stresses are obtained from STAGS models with five stringer bays and from STAGS models with only two stringer bays. For the STAGS models with only two stringer bays the influence of stiffeners along the edges is determined. STAGS predicts significantly higher maximum effective stresses in the two-stringer-bay models in which stiffeners along the edges are not present. None of the PANDA2 or STAGS models, which are both based on thin shell approximations, include the effect of very local stress concentration at the "corner" where a stringer root meets the panel skin. In order to predict the maximum local post-buckling effective stress in an actual fabricated structure, one would have to include a finite fillet radius at a stringer web

root, and one would have to include three-dimensional solid finite elements in both the panel skin and in the part of the stringer in the immediate neighborhood of the root of that stringer. Enough detail is presented here so that PANDA2 and STAGS users can treat this report as a user's manual to explore other cases by analogy.

SUMMARY

An elastic, axially compressed. aluminum, internally ring and stringer stiffened cylindrical shell 130 inches long and with radius equal to 50 inches is first optimized with the use of PANDA2 [1-22]. The internal stiffeners have rectangular cross sections. The height of the rings is constrained to be equal to the height of the stringers. The applied axial resultant, Nx is -1000 lb/in. (Nx = -1000 lb/in is called "the design load".) The factor of safety, FSLOC, for local buckling of the panel skin between adjacent stiffeners is set equal to 0.1 in the PANDA2 model in order that local post-buckling behavior be permitted at an axial load considerably less than the design load, Nx = -1000 lb/in. In the optimum design the ring spacing is 9.7793 inches and the stringer spacing is 2.4705 inches. For the optimized design local buckling occurs at a load factor, EIG(local) = 0.31375 (Nx = -313.75 lb/in), about one third of the design load, Nx = -1000 lb/in. Most of this report is devoted to a study of a small portion of the optimized cylindrical shell with the use of STAGS [23-26]. STAGS finite element models are explored that span only one ring bay and that include either 5 stringer bays or only two stringer bays. The rings at either end of the one-ring-bay are included in the STAGS models. Both curved and flat geometries of this small part of the complete, internally ring and stringer stiffened cylindrical shell are modeled with STAGS. The main purpose of this study is to compare the predictions of PANDA2 and STAGS of post-local-buckling displacement pattern and maximum effective stress at the design load, Nx = -1000 lb/in.

This report is divided into sections and sub-sections and sub-sub-sections as follows:

Section 1.0:
THE PANDA2 MODELS AND PREDICTIONS FOR A CURVED AND FOR A FLAT PANEL
Section 1.1:
PANDA2 Model and Predictions for a Curved Panel (a cylindrical shell)
Section 1.1.1
Input for BEGIN, DECIDE, MAINSETUP, etc, and run stream
Section 1.1.2
Details concerning PANDA2 output for the optimized design
Section 1.1.3
Comments on the PANDA2 predictions for the optimized design
Section 1.2:
PANDA2 Model and Predictions for a One-Ring-Bay Flat Panel
Section 1.2.1:
5-stringer-bay flat panel with one ring bay, including rings
Section 1.2.2;
10-stringer-bay flat panel with one ring bay, including rings

Section 2.0:
MODIFICATIONS TO STAGSUNIT (the program called "stagun.src")
Section 2.1:
Item No. 796 in the File, ...panda2/doc/panda2.news

Section 2.2:
Item No. 797 in the File, ...panda2/doc/panda2.news

Section 3.0:
STAGS PREDICTIONS OF LOCAL BUCKLING AND POST-BUCKLING BEHAVIOR
Section 3.1:
Curved panel with overall axial bending permitted, No edge warping
Section 3.2:
Curved panel with overall axial bending NOT permitted, NO edge warping
Section 3.3:
Curved panel with overall axial bending NOT permitted, YES edge warping
Section 3.4
Flat panel with overall axial bending NOT permitted, NO edge warping
Section 3.4.1:
Flat Panel with 5 Stringer Bays
Section 3.4.2:
Flat Panel with 10 Stringer Bays
Section 3.5
Flat and Curved Panels with 2 Stringer Bays
Section 3.5.1
Flat Panel with 2 Stringer Bays and with stiffeners along the 4 edges
Section 3.5.2
Flat Panel with 2 Stringer Bays and with no stiffeners along the 4 edges
Section 3.5.3
Curved Panel with 2 Stringer Bays and with stiffeners along the 4 edges
Section 3.5.4
Curved Panel with 2 Stringer Bays and with no stiffeners along the 4 edges

Section 4.0
CONCLUSIONS

Section 5.0
REFERENCES

Section 1.0:
THE PANDA2 MODELS AND PREDICTIONS FOR A CURVED AND FOR A FLAT PANEL

Section 1.1:
PANDA2 Model and Predictions for a Curved Panel

Tables 1 - 14 and Figs 1 - 11b pertain to this sub-section. The PANDA2 case is called "allenrngs" after Allen Waters, a Lockheed Martin colleague working at NASA Langley Research Center who inspired the effort reported here.

Section 1.1.1
Input for BEGIN, DECIDE, MAINSETUP, etc, and Run Stream

PANDA2 is used to optimize a complete cylindrical shell. The input data for PANDA2 are listed in the three files, allenrngs.BEG (Table 1), allenrngs.DEC (Table 2), and allenrngs.OPT (Table 3).

The length of the cylindrical shell is 130 inches and its radius is 50 inches. The material properties, as specified in the allenrngs.BEG file (Table 1) are as follows:

```
-----------------------------------------------------------------
    y        $ Is this material isotropic (Y or N)?
0.1010E+08 $ Young's modulus,                    E( 1)
0.3000     $ Poisson's ratio,                   NU( 1)
 3884615.  $ transverse shear modulus,      G13( 1)
       0   $ Thermal expansion coeff.,    ALPHA( 1)
       0   $ residual stress temperature (positive),TEMPTUR( 1)
    n      $ Want to supply a stress-strain "curve" for this mat'l (H)?
    y      $ Want to specify  maximum effective stress ?
 60000.00  $ Maximum allowable effective stress in material type( 1)
    n      $ Do you want to take advantage of "bending overshoot"?
0.1000000  $ weight density (greater than 0!) of material type( 1)
-----------------------------------------------------------------
```

The boundary conditions, as specified in the allenrngs.BEG file, are:

```
-----------------------------------------------------------------
 0 $ Prebuckling: choose 0=bending included; 2=use membrane theory
 0 $ Buckling: choose 0=simple support or 1=clamping
-----------------------------------------------------------------
```

The prebucking bending referred to above is the bending at a ring station and the bending midway between ring stations at a location remote from either end of the shell. Local axial bending in the neighborhoods of the two curved boundaries of a cylindrical shell is not considered by PANDA2 for ring-stiffened shells.

The design load is uniform axial compression, as specified in the allenrngs.OPT file (Table 3):

```
-----------------------------------------------------------------
-1000.00 $ Resultant (e.g. lb/in) normal to the plane of screen, Nx(1)
0.000000 $ Resultant (e.g. lb/in) in the plane of the screen,   Ny(1)
0.000000 $ In-plane shear in load set A,                       Nxy(1)
0.000000 $ Uniform applied pressure [positive upward.See H(elp)], p(1)
-----------------------------------------------------------------
```

The shell is perfect, as specified in the allenrngs.OPT file (Table 3):

```
-----------------------------------------------------------------
0.0 $ Out-of-roundness, Wimpg1=(Max.diameter-Min.diam)/4, Wimpg1(1)
0.0 $ Initial buckling modal general imperfection amplitude, Wimpg2(1)
0.0 $ Initial buckling modal inter-ring imperfection amplitude,Wpan(1)
```

```
0.0E-06 $ Initial local imperfection amplitude (must be positive),Wloc(1)
----------------------------------------------------------------------
```

The factors of safety for general, inter-ring, and local buckling, as specified in the allenrngs.OPT file (Table 3), are as follows:

```
----------------------------------------------------------------------
0.999 $ Factor of safety for general instability, FSGEN(1)
0.999 $ Factor of safety for panel (between rings) instability,FSPAN(1)
0.100 $ Minimum load factor for local buckling (Type H for HELP),FSLOC(1)
1.000 $ Minimum load factor for stiffener buckling (Type H),FSBSTR(1)
1.000 $ Factor of safety for stress, FSSTR(1)
----------------------------------------------------------------------
```

*********************** IMPORTANT NOTE *************************

Notice that the way in which we optimize a panel for service in the locally post-buckled regime is to set the factor of safety for local buckling, FSLOC, equal to a number significantly less than unity. FSLOC equals 0.1 in this example. This is done so that it is unlikely that the local buckling constraint will affect the evolution of the optimum design during executions of SUPEROPT.

****

***************** ANOTHER IMPORTANT NOTE ***************************

In both the PANDA2 and STAGS models the stringers and rings are not connected to each other in any way. At intersections of rings and stringers the rings and stringers are allowed to pass freely through each other as they deform.

****

The starting dimensions given in the file, allenrngs.BEG (Table 1) are:

```
----------------------------------------------------------------------
DIMENSIONS OF  CURRENT  DESIGN...
VARIABLE CURRENT
 NUMBER   VALUE             DEFINITION
   1    5.5000E+00     B(STR):stiffener spacing, b: STR seg=NA, layer=NA
   2    1.8333E+00     B2(STR):width of stringer base, b2 (must be > 0, see
   3    9.8000E-01      H(STR):height of stiffener (type H for sketch), h: S
   4    5.0000E-02 T(1 )(SKN):thickness for layer index no.(1 ): SKN seg=1
   5    9.0000E-02 T(2 )(STR):thickness for layer index no.(2 ): STR seg=3
   6    1.3000E+01      B(RNG):stiffener spacing, b: RNG seg=NA, layer=NA
   7    0.0000E+00     B2(RNG):width of ring base, b2 (zero is allowed): RNG
   8    9.8000E-01      H(RNG):height of stiffener (type H for sketch), h: R
   9    9.0000E-02 T(3 )(RNG):thickness for layer index no.(3 ): RNG seg=3
----------------------------------------------------------------------
```

The following run stream with the use of PANDA2 produces and saves the optimum design and obtains detailed results for that optimum design:

```
----------------------------------------------------------------------
```

```
panda2log  (activate PANDA2 command set)
begin      (execute BEGIN with the use of allenrngs.BEG (Table 1) as
            input)
setup      (PANDA2 sets up template matrices; no input required)
decide     (execute DECIDE with the use of allenrngs.DEC (Table 2) as
            input)
mainsetup  (execute MAINSETUP with the use of allenrngs.OPT (Table 3)
            as input. Note that NPRINT = 0 and ITYPE = 1)
superopt   (run PANDA2 mainprocessor, PANDAOPT, repeatedly in a
            search for a "global" optimum design [5])
chooseplot (choose what to plot vs design iterations. In this
            case plot only the objective vs design iterations (Fig. 1).)
superopt   (run PANDA2 mainprocessor, PANDAOPT, repeatedly in a
            search for a "global" optimum design [5])
chooseplot (choose what to plot vs design iterations. In this
            case plot only the objective vs design iterations (Fig. 2).)
change     (execute CHANGE as a way to save the optimum design. The
            input data for change are listed in allenrngs.CHG (Table 4))
mainsetup  (execute MAINSETUP with the use of allenrngs.OPT (Table 3) as
            input, but with NPRINT = 2 and ITYPE = 2 instead of 0 and 1,
            respectively, as they exist in Table 3)
pandaopt   (execute PANDAOPT to obtain results from PANDA2 for the
            optimized design. The output are listed in the
            allenrngs.OPM file (edited version in Table 5). Highlights
            from Table 5 are included in the text below.)
-------------------------------------------------------------------
```

*********************** IMPORTANT NOTE *******************************
Notice that SUPEROPT was executed twice. It turns out in this particular case that the optimum design at the end of the second execution of SUPEROPT is the same as that at the end of the first execution of SUPEROPT. Note that in order to execute SUPEROPT multiple times the PANDA2 user must follow each execution of SUPEROPT by an execution of CHOOSEPLOT. CHOOSEPLOT resets the total number of design iterations to zero whenever it is executed following a successfully completed execution of SUPEROPT. One can tell if SUPEROPT was successfully executed by looking at the total number of design iterations in the file, allenrngs.OPP. For a successful execution of SUPEROPT this total number of design iterations must exceed 470.
****

The optimum design, as listed near the beginning of the allenrngs.OPM file generated from the last execution of PANDAOPT listed above, is:
```
-------------------------------------------------------------------
 DIMENSIONS OF  CURRENT  DESIGN...
VARIABLE CURRENT
 NUMBER   VALUE            DEFINITION
   1     2.4705E+00      B(STR):stiffener spacing, b: STR seg=NA, layer=NA
   2     8.2342E-01      B2(STR):width of stringer base, b2 (must be > 0, see
   3     8.0436E-01      H(STR):height of stiffener (type H for sketch), h: S
```

```
  4     2.4804E-02 T(1 )(SKN):thickness for layer index no.(1 ): SKN seg=1
  5     7.9480E-02 T(2 )(STR):thickness for layer index no.(2 ): STR seg=3
  6     9.7793E+00     B(RNG):stiffener spacing, b: RNG seg=NA, layer=NA
  7     0.0000E+00    B2(RNG):width of ring base, b2 (zero is allowed): RNG
  8     8.0436E-01     H(RNG):height of stiffener (type H for sketch), h: R
  9     5.8635E-02 T(3 )(RNG):thickness for layer index no.(3 ): RNG seg=3
---------------------------------------------------------------------
```

The optimized objective, as listed in the allenrngs.OPM file, is:

```
---------------------------------------------------------------------
    CURRENT VALUE OF THE OBJECTIVE FUNCTION:
 VAR. STR/ SEG. LAYER    CURRENT
 NO.  RNG  NO.   NO.     VALUE               DEFINITION
            0     0    1.133E+02   WEIGHT OF THE ENTIRE PANEL

  TOTAL WEIGHT OF SKIN                         =   5.0651E+01
  TOTAL WEIGHT OF SUBSTIFFENERS                =   0.0000E+00
  TOTAL WEIGHT OF STRINGERS                    =   5.2843E+01
  TOTAL WEIGHT OF RINGS                        =   9.8484E+00
  SPECIFIC WEIGHT (WEIGHT/AREA) OF STIFFENED PANEL=   5.5504E-03
---------------------------------------------------------------------
```

```
*****************************************************************************
************************* IMPORTANT NOTE *********************************
```
When this study was almost finished **a serious bug was found in SUBROUTINE MODE** (the mode.src library). This bug and its important effect on local post-buckling behavior is described in Item No. 804 of the file, ...panda2/doc/panda2.news. Because of this, the optimized design just listed is not feasible. Therefore, the design just listed was used a starting design and another execution of SUPEROPT was conducted. A new allenrngs.DEC file was used for this new "global" optimization, as follows:

```
--------------------- new input for DECIDE ----------------------------
     n              $ Do you want a tutorial session and tutorial output?
     n              $ Want to use default for thickness decision variables
        3           $ Choose a decision variable (1,2,3,...)
  0.1000000         $ Lower bound of variable no.( 3)
  3.000000          $ Upper bound of variable no.( 3)
     y              $ Any more decision variables (Y or N) ?
        4           $ Choose a decision variable (1,2,3,...)
  0.1000000E-01 $ Lower bound of variable no.( 4)
  0.5000000         $ Upper bound of variable no.( 4)
     y              $ Any more decision variables (Y or N) ?
        5           $ Choose a decision variable (1,2,3,...)
  0.1000000E-01 $ Lower bound of variable no.( 5)
  0.5000000         $ Upper bound of variable no.( 5)
     y              $ Any more decision variables (Y or N) ?
        9           $ Choose a decision variable (1,2,3,...)
  0.2000000E-01 $ Lower bound of variable no.( 9)
```

```
  0.2000000          $ Upper bound of variable no.( 9)
        n            $ Any more decision variables (Y or N) ?
        y            $ Any linked variables (Y or N) ?
            8        $ Choose a linked variable (1,2,3,...)
            3        $ To which variable is this variable linked?
  1.000000           $ Assign a value to the linking coefficient, C(j)
        n            $ Any other decision variables in the linking expression?
        n            $ Any constant C0 in the linking expression (Y or N)?
        n            $ Any more linked variables (Y or N) ?
        n            $ Any inequality relations among variables? (type H)
        y            $ Any escape variables (Y or N) ?
        y            $ Want to have escape variables chosen by default?
-----------------------------------------------------------------
```

In this new allenrngs.DEC file, the stringer spacing and ring spacing are not selected as decision variables and therefore do not change during the new execution of SUPEROPT. In the new allenrngs.DEC file just listed only the height of the stringers (variable 3) and the various thicknesses (variables 4, 5 and 9) are the new decision variables. The height of the rings (variable 8) is linked to the height of the stringers (variable 3). **The stringer spacing remains at 2.4705 inches and the ring spacing remains at 9.7793 inches.** This limitation leads to a slightly heavier-than-optimum design (180 degrees of the cylindrcal shell weighs 116 lbs instead of 115 lbs). The stringer spacing of 2.4705 inches and the ring spacing of 9.7793 inches were not included as decision variables during the new optimization in order to avoid having to re-write large sections of this report because of big differences in the old and new optimum designs and in order to avoid having to re-establish the input files, *.STG, for STAGSUNIT that lead to the STAGS input files, *.bin and *.inp, for STAGS models with finite element meshes the spacing of which varies over the sub-domain of the cylindrical shell to be analyzed with STAGS.

The new optimum design after one execution of SUPEROPT is as follows:
```
------------------------------------------------------------------------
DIMENSIONS OF  CURRENT  DESIGN...
VARIABLE CURRENT
 NUMBER    VALUE                DEFINITION
   1     2.4705E+00     B(STR):stiffener spacing, b: STR seg=NA, layer=NA
   2     8.2342E-01    B2(STR):width of stringer base, b2 (must be > 0, see
   3     8.4714E-01     H(STR):height of stiffener (type H for sketch), h: S
   4     2.4141E-02 T(1 )(SKN):thickness for layer index no.(1 ): SKN seg=1
   5     8.0087E-02 T(2 )(STR):thickness for layer index no.(2 ): STR seg=3
   6     9.7793E+00     B(RNG):stiffener spacing, b: RNG seg=NA, layer=NA
   7     0.0000E+00    B2(RNG):width of ring base, b2 (zero is allowed): RNG
   8     8.4714E-01     H(RNG):height of stiffener (type H for sketch), h: R
   9     6.0060E-02 T(3 )(RNG):thickness for layer index no.(3 ): RNG seg=3
------------------------------------------------------------------------
```

The remainder of this report is based on the optimum design just listed.

The new objective, as listed in the allenrngs.OPM file (Table 5), is:
```
------------------------------------------------------------------------
```

```
      CURRENT VALUE OF THE OBJECTIVE FUNCTION:
  VAR. STR/ SEG. LAYER   CURRENT
  NO.  RNG NO.   NO.     VALUE              DEFINITION
            0     0    1.160E+02   WEIGHT OF THE ENTIRE PANEL

   TOTAL WEIGHT OF SKIN                         =    4.9297E+01
   TOTAL WEIGHT OF SUBSTIFFENERS                =    0.0000E+00
   TOTAL WEIGHT OF STRINGERS                    =    5.6079E+01
   TOTAL WEIGHT OF RINGS                        =    1.0624E+01
   SPECIFIC WEIGHT (WEIGHT/AREA) OF STIFFENED PANEL=    5.6806E-03
  ----------------------------------------------------------------------
```

All the PANDA2 and STAGS results presented here correspond to the new optimum design just listed.
******************** END OF IMPORTANT NOTE *************************

The design margins corresponding to the new optimized design, as listed in the allenrngs.OPM file (Table 5), are as follows:

SUBCASE 1 (corresponding to conditions midway between adjacent rings):

```
  ----------------------------------------------------------------------
   MARGINS FOR CURRENT DESIGN: LOAD CASE NO. 1, SUBCASE NO. 1
   MAR. MARGIN
   NO.  VALUE                   DEFINITION
    1  2.14E+00 Local buckling from discrete model-1.,M=6   axial halfwaves;FS=0.1
    2  2.08E+00 Local buckling from Koiter theory,M=6    axial halfwaves;FS=0.1
    3  7.01E-02 eff.stress:matl=1,SKN,Dseg=2,node=6,layer=1,z=-0.0121; MID.;FS=1.
    4  1.66E+04 stringer popoff margin:(allowable/actual)-1, web 1  MID.;FS=1.
    5  2.07E-01 Hi-axial-wave post-post-buckling of module - 1;   M=12 ;FS=1.
    6  1.69E-02 (m=1   lateral-torsional buckling load factor)/(FS)-1;FS=0.999
    7  5.92E-01 Inter-ring bucklng, discrete model, n=13  circ.halfwaves;FS=0.999
    8  2.05E+00 eff.stress:matl=1,SKN,Iseg=2,at:n=6,layer=1,z=-0.0121;-MID.;FS=1.
    9  9.99E-01 buckling margin stringer Iseg.3 . Local halfwaves=4   .MID.;FS=1.
   10  1.26E+00 buckling margin stringer Iseg.3 . Local halfwaves=4   .NOPO;FS=1.
   11 -4.59E-02 buck.(SAND);simp-support general buck;M=4;N=7;slope=0.;FS=0.999
   12  6.98E+01 buck.(SAND);rolling with smear rings; M=186;N=1;slope=0.;FS=0.1
   13  2.26E+00 buck.(SAND);rolling only of stringers;M=93;N=0;slope=0.;FS=1.4
   14  3.89E+02 (Max.allowable ave.axial strain)/(ave.axial strain) -1; FS=1.
   15  9.00E-05 0.3333 *(Stringer spacing, b)/(Stringer base width, b2)-1;FS=1.
  ----------------------------------------------------------------------
```


SUBCASE 2 (corresponding to conditions at a ring station):

```
  ----------------------------------------------------------------------
   MARGINS FOR CURRENT DESIGN: LOAD CASE NO. 1, SUBCASE NO. 2
   MAR. MARGIN
   NO.  VALUE                   DEFINITION
    1  2.11E+00 Local buckling from discrete model-1.,M=6    axial halfwaves;FS=0.1
    2  2.03E+00 Local buckling from Koiter theory,M=6    axial halfwaves;FS=0.1
    3  1.76E-01 eff.stress:matl=1,SKN,Dseg=2,node=6,layer=1,z=-0.0121; RNGS;FS=1.
```

```
 4  1.73E+04 stringer popoff margin:(allowable/actual)-1, web 1  RNGS;FS=1.
 5  2.44E-01 Hi-axial-wave post-post-buckling of module - 1;   M=12 ;FS=1.
 6  4.37E-03 (m=1   lateral-torsional buckling load factor)/(FS)-1;FS=0.999
 7  6.01E-01 Inter-ring bucklng, discrete model, n=13  circ.halfwaves;FS=0.999
 8  2.12E+00 eff.stress:matl=1,STR,Iseg=3,at:ROOT,layer=1,z=0.;-RNGS;FS=1.
 9  8.57E-01 buckling margin stringer Iseg.3 . Local halfwaves=4  .RNGS;FS=1.
10  6.99E+01 buck.(SAND);rolling with smear rings; M=186;N=1;slope=0.;FS=0.1
11  2.17E+00 buck.(SAND);rolling only of stringers;M=93;N=0;slope=0.;FS=1.4
12  4.14E+02 (Max.allowable ave.axial strain)/(ave.axial strain) -1; FS=1.
--------------------------------------------------------------------------
```

Various STAGS models were set up for the **curved panel**. The PANDA2 processor called STAGSUNIT was used to generate valid input files, *.bin and *.inp, for STAGS. The following files contain input for the PANDA2 processor called STAGSUNIT:

```
-----------------------------------------------------------------------
 allenrngs.superopt1.5bay.480.stg                    (Table 7)  <--this report
 allenrngs.superopt1.5bay.yvariablespacing.480.stg   (Table 8)  <--not reported
 allenrngs.superopt1.5bay.yvariablespacing.410.stg   (Table 9)  <--not reported
 allenrngs.superopt1.5bay.yvariablespacing2.410.stg  (Table 10) <--not reported
 allenrngs.superopt1.5bay.yvariablespacing2.480.stg  (Table 11) <--not reported
 allenrngs.superopt1.5bay.yvariablespacing3.480.stg  (Table 12) <--this report
 allenrngs.superopt1.5bay.yvariablespacing4.480.stg  (Table 13) <--Figs.a4,a5
 allenrngs.superopt1.5bay.480.axialbending.stg       (Table 14) <--this report
-----------------------------------------------------------------------
```

STAGS results corresponding to the three ".stg" files indicated "**this report**" are discussed in sections below. These sections describe predictions from the various STAGS models. The other STAGS models, "not reported", were explored in the previous version of this report that was generated before the bug in SUBROUTINE MODE was discovered (Item 804 in .../panda2/doc/panda2.news). In addition to the tables just identified, which all pertain to STAGS models with five stringer bays, there are tables that pertain to flat panels with 5 stringer bays, 10 stringer bays and 2 stringer bays. These additional tables are cited later. The one STAGS model in which the finite element mesh density varies in both the x and the y coordinate directions (Table 13) is shown in the appendix in Figs. a4 and a5.

The optimum design was next subjected to an ITYPE = 3 analysis with the use of PANDA2. ITYPE = 3 in the *.OPT file (input for MAINSETUP) corresponds to a simulation of a simulated test of the optimized panel under increasing applied loading. The PANDA2 run stream is as follows:

```
--------------------------------------------------------------------------
mainsetup  (execute MAINSETUP with the use of allenrngs.OPT as input
            with NPRINT = 0 and ITYPE = 3 (Table 6))
pandaopt   (execute PANDAOPT to obtain results from PANDA2 for the
            test simulation of the optimized design.)
chooseplot (choose what to plot vs applied load. In this example
            several plots are obtained of various quantities vs
            the applied axial compression, Nx. (Table 6b))
diplot     (obtain the following Postscript files:
 22820 Nov 30 09:40 allenrngs.3.ps (design margins vs Nx,     Fig. 3)
 14522 Nov 30 09:40 allenrngs.4.ps (behaviors vs Nx,          Fig. 4)
```

```
 28874 Nov 30 09:40 allenrngs.5.ps (deformed module vs Nx,     Fig. 5)
 14860 Nov 30 09:40 allenrngs.6.ps (undeformed module),         Fig. 6)
 80589 Nov 30 09:40 allenrngs.7.ps (3-D deformed module,        Fig. 7)
 18441 Nov 30 09:40 allenrngs.8.ps (axial strain vs Nx,         Fig. 8)
 19179 Nov 30 09:40 allenrngs.9.ps ("hoop" strain vs Nx,        Fig. 9)
 18441 Nov 30 09:40 allenrngs.10.ps(in-plane shear strain v Nx,Fig.10)

chooseplot (This time plot only the panel skin axial stiffness C11 vs Nx)
diplot     (obtain the Postscript file for C11(skin) vs Nx)    Fig.11)

(Execute several PANDA2 "fixed design" runs (ITYPE=2 in the *.OPT file)
for the same optimum design but with a series of local buckling modal
imperfections with various amplitudes, Wimp(local). Results are plotted in
Figs. 4b and 11b.)
-------------------------------------------------------------------------
```
******************** END OF SUB-SUB-SECTION 1.1.1 ************************

Section 1.1.2
Details concerning PANDA2 output for the optimized design

Some comments pertaining to this sub-sub-section follow.

Detailed results for the optimized cylindrical shell are listed in Table 5. This is a very long table and therefore may subject the reader to "information overload". Hence, a few highlights are emphasized here:

1. Table 5 was produced with the choice, NPRINT = 2, in the allenrngs.OPT file (input for MAINSETUP). NPRINT = 2 generates lots of output from the execution of the PANDA2 mainprocessor, PANDAOPT, including:

  a. a rather detailed description of what computations PANDA2 performs.
  b. a list of references to the PANDA2, BOSOR4, and STAGS literature.
  c. a summary of the purpose of each of the 28 "CHAPTERs" processed
     during the execution of PANDAOPT.
  d. a list of the current design dimensions.
  e. results pertaining to each of the 28 CHAPTERs.

Output and some discussion from selected CHAPTERs in the long allenrngs.OPM file (Table 5) follow.

2. CHAPTER 4 computes the axisymmetric prebuckling behavior of a ring-stiffened cylindrical shell under:

  a. Load Set A ("eigenvalue" load set)
  b. Load Set B (not "eigenvalue" load set)
  c. Thermal loads, if any

For example, in this case, in which we have only Load Set A, CHAPTER 4 contributes the following output to the allenrngs.OPM file:

```
 ---------------------------------------------------------------------
 PREBUCKLING DEFORMATION OF CYLINDRICAL SHELL BETWEEN RINGS:
  Subcase number                                    ICASE =      1
  Radius of cylindrical shell                           R = -5.0000E+01
  Ring spacing,                                      B(2) =  9.7793E+00
  Axial resultant,                    Nx(Loadset A) = -1.0000E+03
  Hoop  resultant,                    Ny(Loadset A) = -1.0000E-03
  Normal displacement at midbay,                  WMID =  2.4037E-02
  Normal displacement at rings,                  WRING =  2.3756E-02
  Average normal displacement, Wave =-EPSILON(y)*R =  2.3880E-02
  Meridional curvature change at midbay,   WXXMID = -4.6945E-05
  Meridional curvature change at rings,    WXXRNG =  9.3901E-05
  Axial boundary layer length,                     BLL =  2.2670E+01
  Hoop stiffness EA of ring,                  EA(ring) =  5.1388E+05
  Applied normal pressure,          P(Loadset A) =  2.0000E-05
  Shear in web of stringer,                    SHEARX =  0.0000E+00
  Correction to hoop resultant,               DFNYP0 =  9.6487E-01
  Transverse resultant in isogrid web,      POPISO =  0.0000E+00
 -------------------------------------------------------------------
```

There is bending between rings. This case has two sub-cases because the axisymmetric prebuckling conditions midway between rings (SUBCASE 1) are different from those at the ring stations (SUBCASE 2). In this example the prebuckling states at the two axial locations are only slightly different because the rings are weak.

3. CHAPTER 10 computes knockdown factors and prebuckling bending caused by:

  a. a general buckling modal imperfection (CHAPTER 10.1)
  b. an inter-ring buckling modal imperfection (smeared stringers)
     (CHAPTER 10.2).
  c. a local skin/stringer buckling modal imperfection (CHAPTER 10.3)
  d. a summary of imperfection sensitivity predictions (CHAPTER 10.4).

For example, in this case, for which there are no imperfections, the following results pertaining to imperfection sensitivity appear in the allenrngs.OPM file (part of CHAPTER 10.4):

```
 ================================================================
 BUCKLING LOAD FACTORS AND IMPERFECTION SENSITIVITY SUMMARY
 ------------------------------------------------------------
                    LOCAL       INTER-RING       GENERAL
                   BUCKLING      BUCKLING        BUCKLING
 RATIOS OF BUCKLING LOADS FROM ARBOCZ THEORY TO THOSE FROM
 PANDA2 THEORY FOR THE PERFECT STRUCTURE:
    (ARBOCZ/PANDA2):   9.9988E-01   9.8506E-01   1.0000E+00
 ------------------------------------------------------------
 KNOCKDOWN FACTORS FOR IMPERFECTIONS DERIVED FROM
 PANDA2 THEORY VS THOSE FROM ARBOCZ 1992 UPDATE OF KOITERs
 1963 SPECIAL THEORY:
```

```
FROM PANDA2 THEORY:    9.9999E-01    1.0000E+00    1.0000E+00
FROM ARBOCZ THEORY:    1.0000E+00    1.0000E+00    1.0000E+00
THE GOVERNING KNOCKDOWN FACTOR FOR EACH TYPE OF BUCKLING
(LOCAL, INTER-RING, GENERAL) IS SET EQUAL TO THE MINIMUM
KNOCKDOWN FACTOR FOR THAT TYPE OF BUCKLING, REDUCED
FURTHER BY THE RATIO (ARBOCZ/PANDA2) FOR THE PERFECT PANEL
IF THE RATIO (ARBOCZ/PANDA2) IS LESS THAN UNITY:
The ARBOCZ theory is used only if ICONSV=1. ICONSV= 1

 USED NOW IN PANDA2:    9.9987E-01    9.8506E-01    1.0000E+00


 FACTOR APPLIED TO    1.0000E+00 FOR ALTERNATIVE SOLUTION FOR
 GENERAL    BUCKLING WITH DISCRETE STIFFENERS, FKNMLT=  1.0000E+00
 FACTOR APPLIED TO    9.8506E-01 FOR ALTERNATIVE SOLUTION FOR
 INTER-RING BUCKLING WITH DISCRETE STIFFENERS, FKNMLS=  1.0000E+00

 ***NOTE*** IF THERE IS INTERNAL PRESSURE THESE KNOCKDOWN
            FACTORS MAY BE CHANGED AS NOTED BELOW.
 ================================================================
```

4. CHAPTER 11 computes some knockdown factors other than those relating to initial buckling modal imperfections. For example, CHAPTER 11 generates the following output in the allenrngs.OPM file:

```
----------------------------------------------------------------
 In-plane shear and anisotropy are not directly accounted for
 in any of the BOSOR4-type of discretized models. In order to
 compensate for this error, knockdown factors are established
 as given below for various types of buckling. These knockdowns
 account for:
  1. the effect of in-plane shear, and
  2. anisotropy [e.g. C(4,6), C(5,6)] in the panel skin.
 Knockdown factors from PANDA-type analysis are as follows:
    Knockdown factor for general instability=   1.0000E+00
    Knockdown factor for local instability=     9.9999E-01
    Knockdown factor (under hat crippling)=     1.0000E+00
    Knockdown factor for inter-ring buckling=   1.0000E+00
    Knockdown factor for stringer web bucklng=  1.0000E+00
    Knockdown factor for   ring   web bucklng=  1.0000E+00
 Please note that the purpose of these knockdown factors is NOT
 to compensate for initial imperfections.  You can account for
 initial imperfections by assigning amplitudes of local, inter-
 ring, and general imperfections in the forms of the local,
 inter-ring and general buckling modes. And/or you can use
 appropriate factors of safety (different for different
 buckling modes) to compensate for initial imperfections.
--------------------------------------------------------------
```

These additional knockdown factors are 1.0 (no knockdown) because in this particular case there is no

anisotropy nor in-plane shear loading.

5. CHAPTER 14 computes local buckling load factors from the discretized single skin/stringer module model. (See Figs. 5 - 7). For example, CHAPTER 14 contributes the following output to the allenrngs.OPM file:

```
------------------------------------------------------------------------
 BUCKLING LOAD FACTORS FROM BOSOR4-TYPE DISCRETIZED MODEL...
          (skin-stringer discretized module of local buckling)
   AXIAL       BUCKLING          KNOCKDOWN FOR     KNOCKDOWN FOR        BUCKLING
   HALF-      LOAD FACTOR       TRANSVERSE SHEAR IN-PLANE SHEAR      LOAD FACTOR
   WAVES   BEFORE KNOCKDOWN      DEFORMATION        LOADING AND/OR AFTER KNOCKDWN
                                                    ANISOTROPY
     M         EIGOLD               KSTAR              KNOCK    EIGOLD*KSTAR*KNOCK
     5       3.21937E-01        1.00000E+00        9.99993E-01       3.21935E-01
     6       3.14345E-01        1.00000E+00        9.99993E-01       3.14343E-01
     7       3.26322E-01        1.00000E+00        9.99993E-01       3.26320E-01
 Buckling load factor before t.s.d.=  3.1434E-01 After t.s.d.=  3.1375E-01
     6       3.14345E-01        9.98117E-01        9.99993E-01       3.13751E-01
-----------------------------------------------------------------------
```

The local buckling load factors, "EIGOLD", correspond to about one third of the design load, $Nx = -1000.0$ lb/in. For an applied load, $Nx = -100$ lb/in, which is one tenth of the design load, PANDA2 gets a critical eigenvalue of 3.136. STAGS gets a critical linear eigenvalue of 3.368 (Fig. 21).

6. CHAPTER 16 computes the post-local-buckling state of the single discretized skin/stringer module [3,22]. See Figs. 4 and 5 for depictions of how the post-local buckling displacement grows with increasing axial compression, Nx. For example, CHAPTER 16 contributes the following output to the allenrngs.OPM file:

```
------------------------------------------------------------------------
 LOCAL BIFURCATION BUCKLING LOAD FACTOR ESTIMATES
 AND AMPLITUDE Wo OF LOCAL IMPERFECTION, Wo*(buckling mode)
 Critical number of axial half-waves                = 6
 Slope of buckling nodal lines from Koiter Theory, m=  6.30E-03
 Knockdown factor for C44, C45, C55 for transv.shear=  9.98E-01
 Local buckling load Factor from Koiter-type Theory =  3.08E-01
 Load Factor from BOSOR4-type panel module model    =  3.13E-01
 BOSOR4-type load factor without knockdowns for
    effects of anisotropy [e.g. C(4,6)] of the skin,
    transverse shear def., or in-plane shear loading =  3.14E-01
 Amplitude Wo of local imperfection                 =  1.0000E-07

(lines skipped to save space)

 NEWTON ITERATIONS BEGIN IN SUBROUTINE ENERGY
 CALLED FROM SUBROUTINE KOIT2 AT LABEL = 8010.
 PURPOSE IS TO OBTAIN NEW SOLUTION ALLOWING THE AXIAL
 HALFWAVELENGTH OF THE LOCAL POSTBUCKLED PATTERN TO CHANGE.
```

```
 ITER.         UNKNOWNS IN THE LOCAL POSTBUCKLING PROBLEM
  NO.    AMPLITUDE   FLATTENING   NODAL LINE  PI**2*n**2/4L**2 AXIAL HALFWAVLNGTH
            f           a        SLOPE,  m         N          OF BUCKLES,(L/n)
  0    6.28412E-02  -2.15159E-01  2.17492E-02  9.28810E-01    1.62988E+00
  1    5.95259E-02  -2.44126E-01  1.98637E-02  1.13200E+00    1.47638E+00
  2    5.83214E-02  -2.52053E-01  1.93437E-02  1.21452E+00    1.42533E+00
  3    5.81605E-02  -2.52795E-01  1.92756E-02  1.22529E+00    1.41906E+00
  4    5.81580E-02  -2.52805E-01  1.92746E-02  1.22545E+00    1.41897E+00
  CONVERGENCE SUCCESSFUL!

(lines skipped to save space)

 LOCAL DEFORMATION CHARACTERISTICS:
 Average axial strain(not including thermal),EXAVE = -2.5671E-03
 Initial local imperfection amplitude,           Wo=  1.0000E-07
 Slope of local buckling nodal lines in skin     M =  1.9275E-02
 Parameter "a" in the expression f*(phi +a*phi**3) = -2.5280E-01
 Amplitude  f  in the expression f*(phi +a*phi**3) =  5.8158E-02
 Normal displacement amplitude between stringers W =  4.3455E-02
 Number of axial halfwaves at local bifurcation    =     6
 Number of axial halfwaves in postbuckled regime   =  6.8918E+00
 Convergence characteristic,             NOCONV   =  0

(lines skipped to save space)

 NORMALIZED AVERAGE SKIN TANGENT STIFFNESS MATRIX
 (CTAN(i,i)/CX(i,i,1), i=1,2,3) =   4.0366E-01  7.6718E-01  5.5437E-01
 TANGENT POISSON RATIO
 CTAN(1,2)/CTAN(1,1) =  -1.7940E-01
 NORMALIZED AVERAGE (N1skin,N12skn) COUPLING
 CTAN(1,3)/CX(1,1,1) =   3.7729E-03
 NORMALIZED AVERAGE (N2skin,N12skn) COUPLING
 CTAN(2,3)/CX(2,2,1) =   1.0863E-02

  Average tangent stiffnesses of the panel skin
 have been calculated by integration of the local tangent
 stiffnesses, C11TAN, C12TAN, C22TAN, and C33TAN with
 Simpsons rule integration:
 Average axial tangent stiffness,        CTAN(1,1) =  1.1786E+05
 Average (1,2) tangent stiffness,        CTAN(1,2) =  6.2584E+03
 Average hoop  tangent stiffness,        CTAN(2,2) =  2.0540E+05
 Average shear tangent stiffness,        CTAN(3,3) =  5.1945E+04
 These tangent stiffness components affect wide column,
 general instability, and panel instability load factors.
-----------------------------------------------------------------
```

NOTE: The effect of the recently discovered bug in SUBROUTINE MODE was to cause the "flattening" parameter "a" listed above always to be zero or -0.0001. This error had the effect of causing the maximum effective stress in the discretized panel module to be too low and the effective average axial stiffness of the

locally post-buckled panel skin to be too high, leading to a slightly unconservative optimum design in this particular case. After elimination of the bug in SUBROUTINE MODE the "flattening parameter", "a", is now given in CHAPTER 16 by:

```
Parameter "a" in the expression f*(phi +a*phi**3) = -2.5280E-01
```

```
as is listed above.
```

7. CHAPTER 17 computes local stresses and the effective (vonMises) stress in the locally post-buckled discretized skin/stringer single module model. For example, CHAPTER 17 contributes the following output to the allenrngs.OPM file:

```
------------------------------------------------------------------
     EXPLODED VIEW, SHOWING LAYERS and (SEGMENT, NODE) NUMBERS

                              (3,11)
                               !
            Layer No. 1 -----> ! <---------- Layer No. k
                               !
          Layer No. 1-.        !
                       .       !
    Layer No. 1-.        .     !                .-Layer No. 1
            .         .        !               .
            .              .  (3,1)           .
     --------------     ====================   --------------
   (1,1)    .    (1,11)(2,1)   .  (2,6)      (2,11)(4,1)   .    (4,11)
            .                       .                    .
           .                       .                   .
          Layer No. m         Layer No. n     Layer No. m

  STRESSES AT CRITICAL NODES IN SEGMENTS OF MODULE...
 BUCK.  LOCATION  IN  PANEL    WINDING   IN-PLANE STRESSES IN MATL COORDS. MODE OF     VON MISES
 MODE   SEG. NODE LAYER    Z    ANGLE     SIG1        SIG2        SIG12      FAILURE  EFFECTIVE STRESS
 POS     1    1    1 -1.21E-02   0.0 -3.2717E+04 -1.4227E+04  5.9214E+02 no failure   2.8432E+04
 NEG     1    1    1 -1.21E-02   0.0  2.6051E+04  8.5408E+03 -1.7791E+02 no failure   2.3004E+04
 POS     1    1    1  1.21E-02   0.0  2.8417E+04  1.6915E+04 -1.7791E+02 no failure   2.4760E+04
 NEG     1    1    1  1.21E-02   0.0 -3.3113E+04 -1.5061E+04  5.9214E+02 no failure   2.8734E+04

(lines skipped to save space)

 Change local hoop curvature in panel skin at web root
 in order to avoid unconservative hoop bending strain:
 discretized module segment 2, nodal point 6
 curvature change now used at nodal point 6: WDDPB =  3.5424E-01
 post-local-buckling curvatures at the previous three nodal points:
 WDDVAR(I-1,2),WDDVAR(I-2,2),WDDVAR(I-3,2) =  2.8164E-01  2.0903E-01
1.4057E-01

 BUCK.  LOCATION  IN  PANEL    WINDING   IN-PLANE STRESSES IN MATL COORDS. MODE OF     VON MISES
  MODE   SEG. NODE LAYER    Z    ANGLE     SIG1        SIG2        SIG12      FAILURE  EFFECTIVE STRESS
```

```
POS    2    6    1 -1.21E-02    0.0 -1.0927E+04   4.9762E+04 -1.1943E+03 no failure   5.6068E+04
NEG    2    6    1 -1.21E-02    0.0 -3.9439E+04  -4.5280E+04  1.6085E+03 no failure   4.2752E+04
POS    2    6    1  1.21E-02    0.0 -4.1467E+04  -5.1552E+04  1.6085E+03 no failure   4.7404E+04
NEG    2    6    1  1.21E-02    0.0 -1.3030E+04   4.3237E+04 -1.1943E+03 no failure   5.1058E+04
-----------------------------------------------------------------------------------------
```

The string, "POS" means a "positive local post-buckling lobe" and the string, "NEG" means a "negative local post-buckling lobe".

Segment 2, Node 6 is the point in the base under the stringer that corresponds to the intersection of the stringer web root with the panel skin.

Note that the maximum change in "hoop" curvature, **WDDPB equals 0.35424 1/inch**. Right under the stringer (Segment 2, Nodal Point 6) the change in "hoop" curvature is actually zero. However, the absolute value of the "hoop" curvature change often varies steeply in the immediate neighborhood of the stringer. Therefore, in order to avoid the production of unconservative designs, PANDA2 does an extrapolation from circumferentially neighboring nodal points in Segment 2 of the single discretized module model. (Segment 2 is the base under the stringer.) This is how the quantity, **WDDPB = 0.35424 1/inch**, is computed. "**WDDPB**" means "second derivative of the normal displacement "w" with respect to the segment module width-wise coordinate y (WDD) in the Post-Buckling (PB) regime". The two neighboring curvature changes, WDDVAR(I-1,2) and WDDVAR(I-2,2), are used in a linear extrapolation to obtain **WDDPB** at Nodal Point 6 of Segment 2. The PANDA2 prediction of maximum curvature change, **WDDPB = 0.35424 1/inch,** at the design load, Nx=-1000 lb/in, can be compared to the predictions from STAGS at the load factor, PA = 10.0 (which corresponds to the design load, Nx = -1000 lb/in) shown for the curved panel in Fig. 41, and shown for the flat panel in Fig. 58.

In this case the maximum effective stress in the single discretized module occurs (according to PANDA2) at Nodal Point 6 of Segment 2, that is, right under the stringer. In actuality, the maximum effective stress occurs either on one side or on the other side of the stringer and right next to the stringer web root. This is because the stringer imposes a line moment on the panel skin that gives rise to what, with the use of shell theory, becomes a discontinuity in the circumferential change in curvature of the panel skin with respect to the circumferential coordinate y. With the PANDA2 model as just described, the maximum effective stress occurs in this particular case in the panel skin adjacent to the junction between the root of the stringer web and the panel skin. This maximum effective stress (**56068 psi)** occurs for a positive local buckling lobe (POS) and is on the same surface of the panel skin as the stringer web root (thickness coordinate, z=-0.0121 inch). For a negative buckling lobe (NEG) the maximum effective stress is somewhat less, 51058 psi, and occurs on the opposite surface of the panel skin from the stringer web root (thickness coordinate, z=0.0121 inch).

In the STAGS models of the **curved panel** the **maximum effective stress** always occurs (in the case of internal stringers, remember!) in the panel skin on the **opposite surface of the panel skin from the stringer web root**. This is because in curved panels inward buckles have a higher amplitude than outward buckles, and the maximum effective stress always occurs where significant circumferential tension next to the stringer web root is combined with axial compression there. In the STAGS models of the **flat panel** the **maximum effective stress** occurs in the panel skin and **is approximately the same on either surface of the panel skin**.

8. CHAPTER 18 summarizes some prebuckling deformation quantities, computes a "mode-jumping" constraint condition, and lists the unbuckled stiffnesses and locally post-buckled stiffnesses of the discretized

single skin/stringer module model. For example, CHAPTER 18 contributes the following output to the allenrngs.OPM file:

```
---------------------------------------------------------------------
 PANEL OVERALL & LOCAL IMPERFECTIONS AND DEFORMATION
 General out-of-roundness of cylindrical panel,WIMPG1 =  0.0000E+00
 General initial buckling modal imperfection amplitude=  0.0000E+00
 General modified imperfection amplitude, Wimp(global)=  0.0000E+00
 Local   initial imperfection amplitude, Wimp(local)  =  1.0000E-07
 Panel (inter-ring) initial imp. amplt., Wimp(panel)  =  1.0000E-10
 Bowing due to temperature effects,     W(residual)   =  0.0000E+00
 Overall (inter-ring in cyl) bowing from pressure ,Wp =  2.8069E-04
 Inter-ring bowing (flat panel) from pressure, WPRESR =  0.0000E+00
 Maximum local "pillowing" between stringers,  WLPRES =  5.0496E-03
 Inter-ring bowing due to postbucking effects, WDELKP = -3.1286E-03
 Amplitude factor for bowing except from press,AMPLIT =  3.1279E+00
 Amplitude factor for bowing due to pressure,  AMPLT2 =  1.0502E+00
 Amplitude factor for inter-ring bowing,       AMPLT3 =  1.4916E+00
 Eccentricity of application of axial loads,    ECC   =  0.0000E+00
 Midbay normal displacements for a CURVED panel from SUB.SKIN:
 Midbay normal displacement from Load Set A,   WMIDA =  2.4037E-02
 Midbay normal displacement from Load Set B,   WMIDB =  0.0000E+00
 Midbay normal displacement from temperature,  WMIDT =  0.0000E+00
 Total Midbay normal displacement,             WMDTOT =  2.4037E-02

 *** BEGIN SUBROUTINE LOCAL (HI-M POST-POSTBUCKLING SEARCH) ***
  LABEL NO. IN STRUCT= 9360

 BUCKLING LOAD FACTORS FROM BOSOR4-TYPE DISCRETIZED MODEL...
         (skin-stringer discretized module of local buckling)
  AXIAL     BUCKLING          KNOCKDOWN FOR     KNOCKDOWN FOR     BUCKLING
  HALF-    LOAD FACTOR       TRANSVERSE SHEAR   IN-PLANE SHEAR    LOAD FACTOR
  WAVES  BEFORE KNOCKDOWN     DEFORMATION       LOADING AND/OR  AFTER KNOCKDWN
                                                ANISOTROPY
   M        EIGOLD              KSTAR           KNOCK      EIGOLD*KSTAR*KNOCK
   12     1.21547E+00        1.00000E+00       9.99993E-01       1.21546E+00
   13     1.30898E+00        1.00000E+00       9.99993E-01       1.30897E+00
 Buckling load factor before t.s.d.=  1.2155E+00 After t.s.d.=  1.2067E+00
   12     1.21547E+00        9.92758E-01       9.99993E-01       1.20666E+00
 Buckling load factor from SUB. LOCAL, EIGITR(6)=  1.2067E+00
 Number of axial halfwaves between rings,NPP=   12
  **** END SUBROUTINE LOCAL (HI-M POST-POSTBUCKLING SEARCH) ****

(lines skipped to save space)

 *** BEGIN SUBROUTINE DEFCIJ (POST-LOCALLY BUCKLED CS(I,J)) ****
 Effective stiffnesses of undeformed and of
 locally deformed module segments:
                                           Undeformed    Deformed
```

```
Effective axial  stiffness of panel SKIN + BASE =   2.6794E+05   1.1786E+05
Effective hoop   stiffness of panel SKIN + BASE =   2.6794E+05   2.0540E+05
Effective (1,2) stiffness of panel SKIN + BASE =   8.0382E+04   6.2584E+03
Effective axial  stiffness of stringer    WEB    =   8.8888E+05   8.8684E+05
Effective axial  stiffness of stringer   FLANGE =   0.0000E+00   0.0000E+00
Effective shear stiffness of panel SKIN + BASE =   9.3778E+04   5.1945E+04
Effective shear stiffness of stringer    WEB    =   3.1111E+05   3.1111E+05
Effective shear stiffness of stringer   FLANGE =   0.0000E+00   0.0000E+00

 Integrated stringer stiffnesses...
  Effective axial stiffness of stringer,   STIFL =  2.7679E+05
  Effective first moment, Int[STIF*zdz],   STIFM =  1.2049E+05
  Effective second moment,Int[STIF*z**2dz],STIFMM=  6.9005E+04
--------------------------------------------------------------------
```

The quantity:

```
 Total Midbay normal displacement,              WMDTOT =  2.4037E-02
```

is the uniform normal deflection caused by Poisson ratio radial expansion of the cylindrical shell induced by the uniform axial compression, Nx = -1000 lb/in. This component of radial expansion is not included in the plots displayed in Figs. 4 and 4b.

The "HI-M POST-POSTBUCKLING SEARCH" produces the "mode-jumping" constraint condition and corresponding design margin.

9. CHAPTER 20 computes lateral-torsional buckling including the effect of the softer, locally post-buckled skin. For example, CHAPTER 20 contibutes the following output to the allenrngs.OPM file:

```
--------------------------------------------------------------------
 Effective axial length of the panel,          AXLEN2=  9.7793E+00
 LATERAL-TORSIONAL BUCKLING: Search for critical load...
 Number of axial halfwaves=  1; Buckling load factor=  1.0159E+00
(lines skipped)
 Number of axial halfwaves=  2; Buckling load factor=  1.0222E+00
(lines skipped)
 Margin=1.6919E-02 (m=1 lateral-torsional buckling load factor)/(FS)-1;FS=0.999
--------------------------------------------------------------------
```

********************* IMPORTANT NOTE *************************
For the old optimum design (before the bug in SUBROUTINE MODE was discovered), we had in CHAPTER 20 of the old allenrngs.OPM file the following lines:
```
 Number of axial halfwaves=  1; Buckling load factor=  1.0491E+00
(lines skipped)
 Number of axial halfwaves=  2; Buckling load factor=  1.0017E+00
(lines skipped)
 Number of axial halfwaves=  3; Buckling load factor=  9.3392E-01
(lines skipped)
```

```
Margin= 2.7186E-03 (m=2 lateral-torsional buckling load factor)/(FS)-1;FS=0.999
```

Note that although the buckling load factor for 3 axial halfwaves, 0.93392, is less than that for 2 axial halfwaves, PANDA2 judges that the buckling mode corresponding to 3 axial halfwaves is actually a kind of local buckling, not lateral-torsional buckling. PANDA2 uses the following quantity to make this judgment:

```
 AMPLIT.OF BUCKLING MODE AT STRINGER WEB TIP, WTIP  =  4.0764E-01
```

If WTIP is less than 0.5, PANDA2 "decides" that the buckling mode is local skin buckling rather than lateral-torsional buckling of the stringer. This is especially significant in this case because the factor of safety for local skin buckling is FSLOC = 0.1, whereas the factor of safety used for lateral-torsional buckling is the same as that used for general buckling, FSGEN = 0.999, in this case.
```
**********************************************************************
```

10. CHAPTER 26 computes local, inter-ring, and general buckling load factors from PANDA-type models [2], and decides which of these PANDA-type (closed form) predictions to include as design constraints. Some of them are not included because there are other more accurate PANDA2 models used in the same run that supersede the PANDA-type (closed form) models. If a particular PANDA-type buckling model is superseded by a more accurate model of the same buckling phenomenon, PANDA2 prints a messeage such as the following to the allenrngs.OPM file:

```
---------------------------------------------------------------------
 Simple-support inter-ring buckling with smeared stringers
 is not recorded as a margin because this type of buckling
 has been superseded by the results from the discretized
 inter-ring module model, for which inter-ring buckling
 load factors have been computed in the range from n =     1
 to n =    70 circumferential halfwaves.
 The critical simple-support inter-ring buckling model has    3
 circ. half waves, which lies within this range.
---------------------------------------------------------------------
```
In the above excerpt from the allenrngs.OPM file occurs the lines:

```
The critical simple-support inter-ring buckling model has    3
circ. half waves, which lies within this range.
```

Why does the PANDA-type (closed form, [2]) model of inter-ring buckling yield such an unexpectedly low value of number of circumferential waves? The reason is a subtle one and is partly explained by the following output included in the more complete list of the allenrngs.OPM file presented in CHAPTER 26 in Table 5:

```
INTER-RING BUCKLING load factors and (axial, circumfer.) halfwaves:
 Sanders theory is used for these buckling calculations in this case.
 INTER-RING BUCKLING FROM PANDA-TYPE THEORY [1B]
    AFTER KNOCKDOWN FOR t.s.d. AND FOR SMEARED STRINGERS:
 EIGSS =   1.6263E+00(m=  1,n=  14)
 Inter-ring eigenvalue with panel as flat:
 EIGSS2=   1.6525E+00(m=  1,n=   3)
```

The actual number of circumferential waves is 14, as listed above corresponding to the eigenvalue, EIGSS.

However, PANDA2 computes inter-ring buckling eigenvalues for both curved and flat panels, and PANDA2 uses the higher of the two eigenvalues, EIGSS (curved panel) or EIGSS2 (flat panel), as the critical eigenvalue and mode shape for inter-ring buckling. In this particular case the flat panel model predicts a slightly higher eigenvalue, EIGSS2 = 1.6525, than does the curved panel model, EIGSS = 1.6263. Therefore, PANDA2 selects EIGSS2 as the critical inter-ring buckling eigenvalue and mode shape. EIGSS2 is associated with a number of circumferential half waves, n = 3 rather than n = 14.

Corresponding to general buckling, CHAPTER 26 contributes the following output to the allenrngs.OPM file:

```
-------------------------------------------------------------------
general buckling: smeared stiffeners, C11=  3.9634E+05, radius, R= -5.0000E+01
 ******** ENTERING GENSTB: PANDA-type buckling model ********
 PANDA-type buckling theory is described in the journal paper:
 D. Bushnell, "Theoretical basis of the PANDA computer program"
 Computers & Structures, Vol. 27, No. 4, pp. 541-563, 1987
 Also see Items 415 and 443 in ...panda2/doc/panda2.news.

(lines skipped)

 EIGMNC=   1.05E+00   1.05E+00   1.05E+00   1.00E+17   1.00E+17   1.05E+00   1.00E+17
 SLOPEX=   0.00E+00   0.00E+00   0.00E+00   0.00E+00   0.00E+00   0.00E+00   0.00E+00
 MWAVEX=      4          4          4          0          0          4          3
 NWAVEX=      7          7          7          0          0          7          0
 TESTX =   4.84E-01   4.84E-01   1.10E+00   0.00E+00   0.00E+00   4.84E-01   1.00E+01
 Before refinement (before CALL EIG), EIGVAL,CSLOPE=   1.0462E+00   0.0000E+00
  After refinement ( after CALL EIG), EIGVAL,CSLOPE=   1.0462E+00   0.0000E+00

(lines skipped)

 Buckling load factor before t.s.d.=  1.0462E+00 After t.s.d.=  1.0164E+00

(lines skipped)

 General buckling loads AFTER knockdown for t.s.d.
 Number of circumferential halfwaves in buckling pattern=  7.0000E+00
 Buckling load factor BEFORE knockdown for smeared stringers=  1.0164E+00
 Buckling load factor AFTER  knockdown for smeared stringers=  9.5315E-01

(lines skipped)

 General buckling load factor before and after knockdown:
 EIGGEN(before modification by 5 factors below)     =  9.5315E-01
 Knockdown factor from modal imperfection(s)        =  1.0000E+00
 Knockdown factor for smearing rings on cyl. shell  =  1.0000E+00
 Knockup factor to avoid twice accounting for t.s.d.=  1.0000E+00
 1st modifying factor, FKNMOD=1 or 1/(EIG9X*FMDKD9) =  1.0000E+00
 2nd modifying factor, EIGMR9=1 or EIGGNX/EIGGEN    =  1.0000E+00

(lines skipped)
```

```
Margin=-4.5895E-02 buck.(SAND);simp-support generalbuck;M=4;N=7;slope=0.;FS=0.999
-------------------------------------------------------------------------
```

For information on EIGMNC, SLOPEX, MWAVEX, NWAVEX listed above, please see Items 415 and 443 in the file, ...panda2/doc/panda2.news. There a description is provided of the complete search over (MWAVEX, NWAVEX, SLOPEX) for the minimum buckling eigenvalue, EIGMNC.

11. CHAPTER 27 computes the objective function, contributing the following output to the allenrngs.OPM file:

```
---------------------------------------------------------------------
 Objective (weight of PANDA2 model of panel), OBJ =  1.1600E+02
---------------------------------------------------------------------
```

OBJ = 1.1600E+02 is the weight of 180 degrees of the cylindrical shell. In the case of a complete cylindrical shell the PANDA2 user always provides input for a panel that spans 180 degrees of the circumference. Predictions from such a model are generally the same as those for a complete cylindrical shell because there are always an even number of circumferential half-waves over the circumference of a complete (360 degree) cylindrical shell. Therefore, there is always an integral number of half waves over 180 degrees of the circumference.

12. CHAPTER 28 presents a summary of dimensions, loading, and design margins. These have been listed above and will not be repeated here.
****************** END OF SUB-SUB-SECTION 1.1.2 ***************************

Section 1.1.3
Comments on the PANDA2 predictions for the optimized design, curved panel

1. The optimum design at the end of the second execution of SUPEROPT (Fig. 2) is the same as that at the end of the first execution of SUPEROPT (Fig. 1) in this particular case. (This was before correction of the bug in SUB. MODE. The situation is different after correction of the bug. However, note that in this case the optimized weight is not very sensitive to the ring spacing.)

2. Note that in Table 6, the input file, allenrngs.OPT, for test simulation (analysis type, ITYPE = 3), the factor of safety for local buckling has been increased from 0.1 to 0.999. The purpose of this increase is to show in Fig. 3 that the shell buckles locally at about one third of the design load, Nx = -1000 lb/in. During optimization cycles the factor of safety for local buckling is 0.1, as listed in Table 3, FSLOC was set equal to a low number in optimization runs so that the local buckling margin would not influence the evolution of the design.

3. In this case there is no initial imperfection. Therefore, the curve plotted in Fig. 4 has a "corner" near the local bifurcation buckling load. Local buckling occurs at a load factor, 0.31375 (Nx = -313.75 lb/in), as revealed in Comment No. 5 in the previous sub-sub-section (1.1.2). If a local buckling modal imperfection had been present, the curve in Fig. 4 would have exhibited a smooth transition from the "prebuckling" phase to the "postbuckling" phase. Figure 4b shows the influence of a local buckling modal imperfections of various

amplituces on the transition from prebuckling to postbuckling states as predicted by PANDA2.

4. The curve in Fig. 4 was generated neglecting the uniform Poisson ratio radial expansion of the cylindrical shell induced by the uniform axial compression, Nx. This Poisson ratio radial expansion is called "WMDTOT" in the output generated with use of the print index, NPRINT = 2 in the allenrngs.OPT file (Table 5). See Comment No. 8 in sub-sub-section 1.1.2 above.

5. Figure 5 shows the locally post-buckled discretized single module model at several load steps. At the design load, Nx = -1000 lb/in, the hoop curvature change at the junction of the stringer root with the panel skin (**WDDPB = 0.35424** in Comment 7 of sub-subsection 1.1.2) is significantly less than that predicted later by STAGS for the curved panel (Fig.41) but agrees reasonably well with the STAGS prediction for the flat panel (Fig. 58). This difference causes the maximum effective stress predicted by PANDA2 (**56068 psi** at Node 6 of Segment 2 in Comment 7 of sub-sub-section 1.1.2) to be significantly less than that predicted by STAGS for the case in which the initial curvature (1/radius) is included in the STAGS model (Fig. 40). The agreement between predictions by PANDA2 and STAGS is much better if the circumferential curvature is neglected in the STAGS model. (See Fig. 58 for the STAGS prediction of circumferential curvature change and Fig. 57 for the STAGS predition of maximum effective stress for a flat panel with the same skin/stringer module dimensions as those used in the PANDA2 analysis of the curved panel (the optimized dimensions). **The reason for the good agreement between PANDA2 and STAGS for the flat panel is that in PANDA2's model for local post-buckling behavior [3,22], the panel skin in the single discretized module model is assumed to be flat even if the panel is a cylindrical shell.**

6. Figure 6 shows the discretized single module model used in the PANDA2 local buckling and post-buckling analyses. In this particular case we chose the width, b2(str), of the base under the stringer to be equal to one third the stringer spacing, b(str). With the same number of nodal points in each of the four segments of the discretized module, this choice leads to uniform nodal point spacing over the entire width of the panel skin.

7. Figure 7 is an isometric (3-dimensional) view of the single panel module that contains one full axial wavelength of the post-buckling pattern. In this case the local buckling and post-buckling mode has six axial halfwaves between rings, or three full axial waves. Therefore, only one third of the axial length of the panel module is displayed in Fig. 7. In all cases PANDA2 shows only one full axial wavelength in this isometric view of post-local-buckling.

8. Figures 8 - 10 show the three extreme fiber in-plane strain components, epsx (Fig.8, axial strain), epxy (Fig.9, hoop strain), and epsxy (Fig.10, in-plane shear strain) plotted with respect to the applied axial resultant, Nx. The load end-shortening curve in Fig. 27 with the legend, "PANDA2 predictions for Radius = 50 inches" was obtained from the data in Fig. 8 by multiplying the axial strain by the ring spacing, 9.7793 inches, and by expressing the axial load Nx as a load factor, PA = |Nx/100|. The PANDA2 predictions in Figs. 8 and 9 should be compared to the STAGS predictions for the flat panel in Figs. 59 and 60. Note that the PANDA2 prediction of in-plane shear strain (Fig. 10) includes the in-plane shear strain at Nodal Point 1 of discretized module segment 2. (Segment 2 in the single discretized module model includes the third of the panel skin width that contains the root of the stringer web at Nodal Point 6.) The location, Nodal Point 1 of Segment 2, in the PANDA2 discretized skin/stringer module (Figs. 5 – 7) is fairly close to where STAGS predicts the maximum post-buckling in-plane shear strain to occur in the flat panel, as is displayed in the STAGS model of the flat panel skin in Fig. a3 of the appendix. The PANDA2 prediction agrees well with the STAGS prediction for the flat panel.

9. Figure 11 is a plot of the normalized axial tangent stiffness of the panel skin, Ctan11/C011, as a function of axial compression, Nx. C011 is the axial stiffness, C(1,1) (lb/in), of the undeformed skin. Local buckling occurs at a load factor, 0.31375 (Nx = -313.75 lb/in), as revealed in Comment No. 5 in the previous sub-sub-section (1.1.2). Note that PANDA2 obtains the "classical" prediction for the post-locally-buckled axial stiffness of a flat plate: approximately half the axial stiffness of the unbuckled plate and fairly constant with axial compression increasing above the local bifurcation buckling load. There is a sharp "corner" at Nx = -313.75 lb/in because there is no local buckling modal imperfection. If there were a local buckling modal imperfection there would exist a smooth transition from the prebuckled state to the post- buckled state. Figure 11b shows the influence of local buckling modal imperfections of various amplitudes on the transition from prebuckling to postbuckling states.

***************** END OF SUB-SUB-SECTION 1.1.3 ***************************

********************** END OF SECTION 1.1 *****************************

Section 1.2:
PANDA2 Model and Predictions for a One-Ring-Bay Flat Panel

The purpose of this sub-section is to determine the effect of the curvature of the panel on results obtained from PANDA2.

Section 1.2.1:
5-stringer-bay flat panel with one ring bay, including rings

Tables 15 - 20 and Figs. 12 - 20 and Fig. 62 pertain to this section.

The panel is not re-optimized. The axial length of the flat panel is now equal to one ring spacing, 9.7793 inches, and the width of the flat panel is equal to five stringer bays, 12.3525 inches. The "local" dimensions are the same as those for the optimized curved panel (after elimination of the bug in SUBROUTINE MODE), as follows:

```
------------------------------------------------------------------------
 DIMENSIONS OF  CURRENT  DESIGN...
VARIABLE CURRENT
 NUMBER   VALUE               DEFINITION
 1      2.4705E+00     B(STR):stiffener spacing, b: STR seg=NA, layer=NA
 2      8.2342E-01    B2(STR):width of stringer base, b2 (must be > 0, see
 3      8.4714E-01     H(STR):height of stiffener (type H for sketch), h: S
 4      2.4141E-02 T(1 )(SKN):thickness for layer index no.(1 ): SKN seg=1
 5      8.0087E-02 T(2 )(STR):thickness for layer index no.(2 ): STR seg=3
 6      9.7793E+00     B(RNG):stiffener spacing, b: RNG seg=NA, layer=NA
 7      0.0000E+00    B2(RNG):width of ring base, b2 (zero is allowed): RNG
 8      8.4714E-01     H(RNG):height of stiffener (type H for sketch), h: R
 9      6.0060E-02 T(3 )(RNG):thickness for layer index no.(3 ): RNG seg=3
------------------------------------------------------------------------
```

The run stream to obtain PANDA2 predictions for the 5-stringer-bay flat panel is as follows:

```
-----------------------------------------------------------------
panda2log  (activate PANDA2 command set)
begin      (execute BEGIN with the use of allenflat.BEG (Table 15) as
            input)
setup      (PANDA2 sets up template matrices; no input required)
decide     (execute DECIDE with the use of allenflat.DEC (Table 16) as
            input)
mainsetup  (execute MAINSETUP with the use of allenflat.OPT as input
            with NPRINT = 2 and ITYPE = 2 (Table 17))
pandaopt   (execute PANDAOPT to obtain results from PANDA2 for the
            optimized design. The output data are listed in the
            allenflat.OPM file (Table 18).)
-----------------------------------------------------------------
```

The objective, as listed in the allenflat.OPM file (Table 18), is:
```
-----------------------------------------------------------------
    CURRENT VALUE OF THE OBJECTIVE FUNCTION:
 VAR. STR/ SEG. LAYER   CURRENT
 NO.  RNG  NO.  NO.      VALUE                 DEFINITION
            0    0    6.862E-01   WEIGHT OF THE ENTIRE PANEL

  TOTAL WEIGHT OF SKIN                           =    2.9162E-01
  TOTAL WEIGHT OF SUBSTIFFENERS                  =    0.0000E+00
  TOTAL WEIGHT OF STRINGERS                      =    3.3174E-01
  TOTAL WEIGHT OF RINGS                          =    6.2849E-02
  SPECIFIC WEIGHT (WEIGHT/AREA) OF STIFFENED PANEL=   5.6806E-03
-----------------------------------------------------------------
```
Note that the weight, 0.6862 lb, is a lot less than that given for the curved panel, 116.0 lb, because only 5
stringer bays and one ring bay are included in the PANDA2 model of the flat panel.

The design margins corresponding to the "optimized" design, as listed in the allenflat.OPM file (Table 18), are
as follows:

SUBCASE 1 (corresponding to conditions midway between adjacent rings):
```
-----------------------------------------------------------------
 MARGINS FOR CURRENT DESIGN: LOAD CASE NO. 1, SUBCASE NO. 1
 MAR. MARGIN
 NO.  VALUE                 DEFINITION
  1  2.20E+00 Local buckling from discrete model-1.,M=6   axial halfwaves;FS=0.1
  2  2.14E+00 Local buckling from Koiter theory,M=6   axial halfwaves;FS=0.1
  3  1.13E-01 eff.stress:matl=1,SKN,Dseg=2,node=6,layer=1,z=0.0121; MID.;FS=1.
  4  1.67E+04 stringer popoff margin:(allowable/actual)-1, web 1  MID.;FS=1.
  5  2.10E+00 eff.stress:matl=1,STR,Iseg=3,at:TIP,layer=1,z=0.;-MID.;FS=1.
  6  2.06E-01 Hi-axial-wave post-post-buckling of module - 1;   M=12 ;FS=1.
  7  1.99E-01 (m=2   lateral-torsional buckling load factor)/(FS)-1;FS=0.999
  8  2.10E+00 eff.stress:matl=1,STR,Iseg=3,at:TIP,layer=1,z=0.;-MID.;FS=1.
  9  1.01E+00 buckling margin stringer Iseg.3 . Local halfwaves=4  .MID.;FS=1.
 10  3.38E+01 buckling margin   ring   Iseg.3 . Local halfwaves=1  .MID.;FS=1.
```

```
11  1.27E+00 buckling margin stringer Iseg.3 . Local halfwaves=4  .NOPO;FS=1.
12  3.38E+01 buckling margin  ring  Iseg.3 . Local halfwaves=1  .NOPO;FS=1.
13  7.03E-01 buck.(SAND);simp-support smear string;M=1;N=1;slope=0.;FS=0.999
14  2.51E+00 buck.(SAND);simp-support general buck;M=1;N=1;slope=0.;FS=0.999
15  7.03E-01 buck.(SAND);rolling with smear string;M=1;N=1;slope=0.;FS=0.999
16  7.04E+01 buck.(SAND);rolling with smear rings; M=14;N=1;slope=0.;FS=0.1
17  2.26E+00 buck.(SAND);rolling only of stringers;M=7;N=0;slope=0.;FS=1.4
18  3.87E+02 (Max.allowable ave.axial strain)/(ave.axial strain) -1; FS=1.
-------------------------------------------------------------------------
```

There is no SUBCASE 2 because the panel is flat. Notice that the design margin for general buckling, Margin No. 14 = 2.51, is different from the margin for general buckling in the curved panel. With the flat panel of axial length equal to the ring spacing, axial length = 9.7793 inches, what is called "general buckling" for the flat panel in this particular case is actually buckling between adjacent rings (with the rings smeared out), whereas with the curved panel general buckling is buckling over the entire axial length, 130 inches, of the curved cylindrical shell. Also, the width of the flat panel, 12.3525 inches, is a lot less than the "width", pi x radius = 157.1 inches, of the curved panel. For the curved panel, allenrngs, the inter-ring buckling margin is listed in Table 5 as Margin number 7:

```
 7  5.92E-01 Inter-ring bucklng, discrete model, n=13 circ.halfwaves;FS=0.999
```

Why is this inter-ring buckling margin so much less than the general buckling margin for the flat panel, that is:

```
14  2.51E+00 buck.(DONL);simp-support general buck;M=1;N=1;slope=0.;FS=0.999
```

It is because in the computation of the general buckling margin of the flat panel, Margin No. 14 = 2.51, the stiffness of the rings is included (smeared out), whereas in the inter-ring buckling margin for the of the curved panel, Margin No. 7 = 0.592, the stiffness of the rings is not included but the rings are replaced by simple support end conditions. The inter-ring buckling phenomenon in the curved panel is simulated in the one-ring-bay model of the flat panel by the two margins:

```
13  7.03E-01 buck.(SAND);simp-support smear string;M=1;N=1;slope=0.;FS=0.999
15  7.03E-01 buck.(SAND);rolling with smear string;M=1;N=1;slope=0.;FS=0.999
```

listed just above in the table of margins for the flat panel.

Two STAGS models were set up for the 5-stringer-bay flat panel. The PANDA2 processor called STAGSUNIT was used to generate valid input files, *.bin and *.inp, for STAGS. The following files contain input for the PANDA2 processor called STAGSUNIT:

```
-----------------------------------------------------------------------
 allenflat.superopt1.5bay.yvariablespacing3.480.stg        (Table 19)
 allenflat.superopt1.5bay.yvariablespacing3.940.stg        (Table 20)
-----------------------------------------------------------------------
```

STAGS results corresponding to the first of these two ".stg" files are discussed in a section below which describes predictions from the various STAGS models. NOTE: The STAGS model with the 940 finite elements ran without error, but the STAGS post-processors did not permit the plotting of effective stress. Therefore, Table 20 is not referred to again in this report.

The flat panel design was next subjected to an ITYPE = 3 analysis type with the use of PANDA2. ITYPE = 3 in the *.OPT file (input for MAINSETUP) corresponds to a simulation of a test of the optimized panel under increasing applied loading. The PANDA2 run stream is as follows:

```
--------------------------------------------------------------------
mainsetup   (execute MAINSETUP with the use of allenflat.OPT as input
             with NPRINT = 0 and ITYPE = 3 (Table 6, except that
             "Axial halfwavelength of typical general buckling mode"
             is given by 9.7793 instead of 130.0))
pandaopt    (execute PANDAOPT to obtain results from PANDA2 for the
             test simulation of the optimized design.)
chooseplot (choose what to plot vs applied load. In this example
             several plots are obtained of various quantities vs
             the applied axial compression, Nx. (Table 6b))
diplot      (obtain the following Postscript files:
 20501 Nov 30 09:40 allenflat.3.ps (design margins vs Nx,     Fig.12)
 14265 Nov 30 09:40 allenflat.4.ps (behaviors vs Nx,          Fig.13)
 28870 Nov 30 09:40 allenflat.5.ps (deformed module vs Nx,    Fig.14)
 14860 Nov 30 09:40 allenflat.6.ps (undeformed module),       Fig.15)
 80589 Nov 30 09:40 allenflat.7.ps (3-D deformed module,      Fig.16)
 18439 Nov 30 09:40 allenflat.8.ps (axial strain vs Nx,       Fig.17)
 19185 Nov 30 09:40 allenflat.9.ps ("hoop" strain vs Nx,      Fig.18)
 18441 Nov 30 09:40 allenflat.10.ps(in-plane shear strain v Nx,Fig.19)

chooseplot (This time plot only the number of axial halfwaves vs Nx)
diplot      (obtain Postscript file for axial halfwaves vs Nx)  Fig.20)
----------------------------------------------------------------------
```

Figures 12 - 19 are analogous to Figs. 3 - 10 for the curved panel. Note that the locally post-buckled states of the flat panel are very close to those of the curved panel. The maximum curvature change in the flat panel at the design load, Nx = -1000 lb/in, is recorded in the allenflat.OPM file (with NPRINT = 2 in the allenflat.OPT file) as follows;

```
-------------------------------------------------------------------
 Change local hoop curvature in panel skin at web root
 in order to avoid unconservative hoop bending strain:
 discretized module segment 2, nodal point 6
 curvature change now used at nodal point 6: WDDPB =  3.5127E-01
 post-local-buckling curvatures at the previous three nodal points:
 WDDVAR(I-1,2),WDDVAR(I-2,2),WDDVAR(I-3,2) =  2.7792E-01  2.0456E-01
1.3616E-01
-------------------------------------------------------------------
```

Compare the above numbers for the flat panel with those listed under Comment No. 7 in sub-sub-section 1.1.2 (curved panel):

```
-------------------------------------------------------------------
 Change local hoop curvature in panel skin at web root
 in order to avoid unconservative hoop bending strain:
```

```
 discretized module segment 2, nodal point 6
 curvature change now used at nodal point 6: WDDPB =  3.5424E-01
 post-local-buckling curvatures at the previous three nodal points:
 WDDVAR(I-1,2),WDDVAR(I-2,2),WDDVAR(I-3,2) =  2.8164E-01  2.0903E-01
 1.4057E-01
```

The maximum effective stress in the flat panel occurs at Nodal Point 6 in Segment 2 of the discretized module, as listed in the allenflat.OPM file obtained with NPRINT = 2 in the allenflat.OPT file (flat panel) :

```
 STRESSES AT CRITICAL NODES IN SEGMENTS OF MODULE...
```

BUCK.	LOCATION		IN	PANEL	WINDING	IN-PLANE STRESSES IN MATL COORDS.			MODE OF	VON MISES
MODE	SEG.	NODE	LAYER	Z	ANGLE	SIG1	SIG2	SIG12	FAILURE	EFFECTIVE STRESS
POS	2	6	1	-1.21E-02	0.0	-1.1909E+04	4.6762E+04	-1.1736E+03	no failure	**5.3755E+04**
NEG	2	6	1	-1.21E-02	0.0	-4.0181E+04	-4.7476E+04	1.5878E+03	no failure	4.4366E+04
POS	2	6	1	1.21E-02	0.0	-4.0238E+04	-4.7155E+04	1.5878E+03	no failure	4.4191E+04
NEG	2	6	1	1.21E-02	0.0	-1.2037E+04	4.6846E+04	-1.1736E+03	no failure	**5.3921E+04**

Compare the above numbers for the flat panel with those listed under Comment No. 7 in sub-sub-section 1.1.2 (curved panel):

BUCK.	LOCATION		IN	PANEL	WINDING	IN-PLANE STRESSES IN MATL COORDS.			MODE OF	VON MISES
MODE	SEG.	NODE	LAYER	Z	ANGLE	SIG1	SIG2	SIG12	FAILURE	EFFECTIVE STRESS
POS	2	6	1	-1.21E-02	0.0	-1.0927E+04	4.9762E+04	-1.1943E+03	no failure	**5.6068E+04**
NEG	2	6	1	-1.21E-02	0.0	-3.9439E+04	-4.5280E+04	1.6085E+03	no failure	4.2752E+04
POS	2	6	1	1.21E-02	0.0	-4.1467E+04	-5.1552E+04	1.6085E+03	no failure	4.7404E+04
NEG	2	6	1	1.21E-02	0.0	-1.3030E+04	4.3237E+04	-1.1943E+03	no failure	**5.1058E+04**

*********************** IMPORTANT NOTE **************************
The PANDA2 results for the locally post-buckled states of the flat and curved panels are close to eachother because the local post-buckling theory in PANDA2 is based on a model in which the single discretized module is FLAT. This critical approximation used by PANDA2 would be too crude if the stringer spacing were not very, very small compared to the radius of the cylindrical panel. Fortunately, in most OPTIMIZED designs the stringer spacing IS very, very small compared to the panel radius. Hence, this critical approximation used by PANDA2 leads to predictions that are not horribly far off the mark for curved axially stiffened panels optimized by PANDA2.

In the present case the biggest discrepancy between predictions by **PANDA2** and predictions by STAGS for the curved panel occurs for the maximum effective stress. For the curved panel PANDA2 predicts a maximum effective stress, **56068 psi**, on the inner surface of the panel skin (thickness coordinate, z = -0.012 inch) and a somewhat lower effective stress, 51058 psi, on the outer surface of the panel skin (thickness coordinate, z = +0.0121 inch). The maximum effective stress predicted by the **STAGS** model of the curved panel is displayed in Fig. 40, which shows that the maximum effective stress at the design load, PA = 10.0 (Nx = -1000 lb/in), is close to **70000 psi** and occurs at what is called in Fig. 40 the "Top" fiber. In this STAGS model the "Top" fiber is the outer surface of the panel skin, that is, the opposite skin surface from that to which the internal stringer is attached.

For the flat panel, **PANDA2** predicts a maximum effective stress that is approximately the same, **53921 psi,** on

either surface of the panel skin. PANDA2 and STAGS predictions are in reasonably good agreement for the flat panel. Figure 57 shows the maximum effective stress versus appled load factor, PA, for the finite element which contains the maximum effective stress. At the design load, PA = 10.0, **STAGS** predicts a maximum effective stress close to **60000 psi** for the flat panel. This maximum occurs in the panel skin at what in Fig. 57 is called the "Bottom" fiber. In this particular STAGS model the "Bottom" fiber is the fiber on the opposite surface of the panel skin from that to which the stringer is attached. However, Figures 54 and 55 demonstrate that the STAGS prediction of maximum effective stress in the flat panel skin is approximately the same for both inner and outer extreme fibers of the panel skin. This prediction is in good agreement with that from PANDA2 for the flat panel: 53755 psi for the skin surface to which the stringer is attached and 53921 psi for the opposite skin surface, as listed above.

The discrepancy between PANDA2 and STAGS predictions of maximum effective stress in the curved panel is caused mainly by the discrepancy in the prediction of the maximum change in circumferential ("hoop") curvature by PANDA2 and by STAGS. For the curved panel STAGS predicts a maximum circumferential curvature change of about 0.46 1/inch (Fig. 41) while PANDA2 predicts WDDPB = 0.354 1/inch. For the flat panel STAGS predicts a maximum cirumferential curvature change of about 0.38 1/inch (Fig. 58) while PANDA2 predicts WDDPB =0.351 1/inch.

These predictions from both PANDA2 and STAGS correspond to thin shell models, not to models that use solid elements. Note that in an actual fabricated panel there would be fillet radii where the stringer web root meets the panel skin. These fillet radii would presumably be generous enough to reduce the maximum effective stress well below the yield stress. Another way substantially to reduce the maximum effective stress is to provide a faying flange under each stringer that is tapered in the circumferential direction. (PANDA2 cannot handle tapered faying flanges.)
****

Figure 20 shows PANDA2's prediction of the change in local post-buckling axial wavelength as a function of the applied axial compression. As the axial compression increases above the local bifurcation buckling load (Nx = -313.75 lb/in) the number of axial half waves between rings increases smoothly, according to PANDA2. That is, the axial wavelength of the buckles decreases smoothly. **This axial wavelength shortening is smooth in the PANDA2 model because the PANDA2 local post-buckling model [3,22] disregards the presence of x-boundaries, that is, boundaries at x = 0 and at x = L,** where L is the axial length of the portion of the panel being considered for analysis. (L = 9.7793 inches, the ring spacing, in this particular case.) In an actual panel, as modeled by STAGS for example, the local post-buckling wavelength often cannot decrease in a smooth manner because the axial length of the STAGS model is finite. This constraint on the local post-buckling behavior often leads to "mode jumping", usually a dynamic phenomenon that involves a sudden change in the number of axial halfwaves in the local post-buckling pattern. An example of this behavior is provided in the section pertaining to predictions by STAGS for a flat, five-stringer-bay panel (Figs. 47-52).

Figure 62 shows a comparison of PANDA2 predictions for curved and flat panels. As expected, the depths of the local buckles in the panel skin are slightly greater for the curved panel than for the flat panel. The quantity, WMDTOT, referred to in the two legends pertaining to the curved panel, is the uniform Poisson ratio radial expansion induced by the uniform axial compression. WMDTOT is given in sub-sub-section 1.1.2 as WMDTOT = 2.4037E-02 inches. (See Comment No. 8 in 1.1.2). Although PANDA2 always assumes in its local post-buckling analysis that the panel skin is flat, this figure exhibits different results for the curved and the flat panel. Why is that? The difference is a consequence of the different prebuckling states of the curved and flat

panels. A small hoop compression, Ny, is generated in the panel skin in the curved panel which is not present in the flat panel. This small Ny [Ny is approximately –25 lb/in at the design load, Nx = -1000 lb/in (PA = 10.0)] results from the fact that the rings constrain the uniform Poisson ratio outward radial expansion induced by the axial compression. Ny in the panel skin is essentially zero in the flat panel.
******************* END OF SUB-SUB-SECTION 1.2.1 **********************

Section 1.2.2:
10-stringer-bay flat panel with one ring bay, including rings

Tables 21 - 23 pertain to this section.

The panel is not re-optimized. The axial length of the flat panel is still equal to one ring spacing, 9.7793 inches, and the width of the flat panel is equal to ten stringer bays: 24.705 inches. The "local" dimensions are the same as those for the optimized curved panel and for the 5-stringer-bay panel, as follows:

```
------------------------------------------------------------------------
  DIMENSIONS OF   CURRENT   DESIGN...
VARIABLE CURRENT
 NUMBER    VALUE                 DEFINITION
  1      2.4705E+00      B(STR):stiffener spacing, b: STR seg=NA, layer=NA
  2      8.2342E-01     B2(STR):width of stringer base, b2 (must be > 0, see
  3      8.4714E-01      H(STR):height of stiffener (type H for sketch), h: S
  4      2.4141E-02 T(1 )(SKN):thickness for layer index no.(1 ): SKN seg=1
  5      8.0087E-02 T(2 )(STR):thickness for layer index no.(2 ): STR seg=3
  6      9.7793E+00      B(RNG):stiffener spacing, b: RNG seg=NA, layer=NA
  7      0.0000E+00     B2(RNG):width of ring base, b2 (zero is allowed): RNG
  8      8.4714E-01      H(RNG):height of stiffener (type H for sketch), h: R
  9      6.0060E-02 T(3 )(RNG):thickness for layer index no.(3 ): RNG seg=3
------------------------------------------------------------------------
```

The run stream to obtain PANDA2 predictions for the 10-stringer-bay flat panel is as follows:

```
------------------------------------------------------------------------
panda2log  (activate PANDA2 command set)
begin      (execute BEGIN with the use of allenflat3.BEG (Table 21) as
            input)
setup      (PANDA2 sets up template matrices; no input required)
decide     (execute DECIDE with the use of allenflat3.DEC (Table 16) as
            input)
mainsetup  (execute MAINSETUP with the use of allenflat3.OPT as input
            with NPRINT = 2 and ITYPE = 2 (Table 17))
pandaopt   (execute PANDAOPT to obtain results from PANDA2 for the
            optimized design. The output data are listed in the
            allenflat3.OPM file (Table 22).)
------------------------------------------------------------------------
```

The objective, as listed in the allenflat3.OPM file (Table 22), is:

```
----------------------------------------------------------------------
   CURRENT VALUE OF THE OBJECTIVE FUNCTION:
 VAR. STR/ SEG. LAYER   CURRENT
 NO.  RNG  NO.   NO.     VALUE              DEFINITION
            0     0    1.372E+00   WEIGHT OF THE ENTIRE PANEL

  TOTAL WEIGHT OF SKIN                          =    5.8324E-01
  TOTAL WEIGHT OF SUBSTIFFENERS                 =    0.0000E+00
  TOTAL WEIGHT OF STRINGERS                     =    6.6348E-01
  TOTAL WEIGHT OF RINGS                         =    1.2570E-01
  SPECIFIC WEIGHT (WEIGHT/AREA) OF STIFFENED PANEL=   5.6806E-03
----------------------------------------------------------------------
```

Note that the weight, 1.372 lb, is twice that of the 5-stringer-bay flat panel, 0.6862 lb, because this flat panel is twice as wide as the 5-stringer-bay flat panel.

The design margins corresponding to the "optimized" design, as listed in the allenflat3.OPM file (Table 22), are as follows:

SUBCASE 1 (corresponding to conditions midway between adjacent rings):

```
----------------------------------------------------------------------------
 MARGINS FOR CURRENT DESIGN: LOAD CASE NO. 1, SUBCASE NO. 1
 MAR. MARGIN
 NO.  VALUE                 DEFINITION
  1  2.20E+00 Local buckling from discrete model-1.,M=6   axial halfwaves;FS=0.1
  2  2.14E+00 Local buckling from Koiter theory,M=6    axial halfwaves;FS=0.1
  3  1.13E-01 eff.stress:matl=1,SKN,Dseg=2,node=6,layer=1,z=0.0121; MID.;FS=1.
  4  1.67E+04 stringer popoff margin:(allowable/actual)-1, web 1  MID.;FS=1.
  5  2.10E+00 eff.stress:matl=1,STR,Iseg=3,at:TIP,layer=1,z=0.;-MID.;FS=1.
  6  2.06E-01 Hi-axial-wave post-post-buckling of module - 1;   M=12 ;FS=1.
  7  1.99E-01 (m=2   lateral-torsional buckling load factor)/(FS)-1;FS=0.999
  8  2.10E+00 eff.stress:matl=1,STR,Iseg=3,at:TIP,layer=1,z=0.;-MID.;FS=1.
  9  1.01E+00 buckling margin stringer Iseg.3 . Local halfwaves=4  .MID.;FS=1.
 10  3.38E+01 buckling margin   ring   Iseg.3 . Local halfwaves=1  .MID.;FS=1.
 11  1.27E+00 buckling margin stringer Iseg.3 . Local halfwaves=4  .NOPO;FS=1.
 12  3.38E+01 buckling margin   ring   Iseg.3 . Local halfwaves=1  .NOPO;FS=1.
 13  6.16E-01 buck.(SAND);simp-support smear string;M=1;N=1;slope=0.;FS=0.999
 14  1.93E+00 buck.(SAND);simp-support general buck;M=1;N=1;slope=0.;FS=0.999
 15  6.16E-01 buck.(SAND);rolling with smear string;M=1;N=1;slope=0.;FS=0.999
 16  7.04E+01 buck.(SAND);rolling with smear rings; M=14;N=1;slope=0.;FS=0.1
 17  2.26E+00 buck.(SAND);rolling only of stringers;M=7;N=0;slope=0.;FS=1.4
 18  3.87E+02 (Max.allowable ave.axial strain)/(ave.axial strain) -1; FS=1.
 19  8.99E-05 0.3333 *(Stringer spacing, b)/(Stringer base width, b2)-1;FS=1.
----------------------------------------------------------------------------
```

There is no SUBCASE 2 because the panel is flat. For the 5-stringer-bay flat panel the general buckling margin is:

```
 14  2.51E+00 buck.(DONL);simp-support general buck;M=1;N=1;slope=0.;FS=0.999
```

whereas for the 10-stringer-bay flat panel the general buckling margins is:

```
14   1.93E+00 buck.(SAND);simp-support general buck;M=1;N=1;slope=0.;FS=0.999
```

The two inter-ring buckling margins for the 5-stringer-bay flat panel are:

```
13   7.03E-01 buck.(SAND);simp-support smear string;M=1;N=1;slope=0.;FS=0.999
15   7.03E-01 buck.(SAND);rolling with smear string;M=1;N=1;slope=0.;FS=0.999
```

whereas for the 10-stringer-bay flat panel the corresponding margins are:

```
13   6.16E-01 buck.(SAND);simp-support smear string;M=1;N=1;slope=0.;FS=0.999
15   6.16E-01 buck.(SAND);rolling with smear string;M=1;N=1;slope=0.;FS=0.999
```

The margins differ for the 5-stringer-bay and 10-stringer-bay flat panel models because the inter-ring buckling load factor is greater for the narrower panel than for the wider panel, as follows:

5-stringer-bay flat panel:
```
 Buckling load factor BEFORE knockdown for smeared stringers=  3.3819E+00
 Buckling load factor AFTER  knockdown for smeared stringers=  1.7009E+00
```

10-stringer-bay flat panel:
```
 Buckling load factor BEFORE knockdown for smeared stringers=  3.2172E+00
 Buckling load factor AFTER  knockdown for smeared stringers=  1.6146E+00
```

One STAGS model was set up for the 10-stringer-bay flat panel. The PANDA2 processor called STAGSUNIT was used to generate valid input files, *.bin and *.inp, for STAGS. The following file contains input for the PANDA2 processor called STAGSUNIT:
```
-----------------------------------------------------------------------
  allenflat3.superopt1.10bay.yvariablespacing3.480.stg     (Table 23)
-----------------------------------------------------------------------
```

STAGS results corresponding to this ".stg" file are discussed in a section below which describes predictions from the STAGS model of a 10-stringer-bay flat panel.

****************** END OF SUB-SUB-SECTION 1.2.1 **********************
********************* END OF SUB-SECTION 1.2 ************************
************************** END OF SECTION 1.0 **********************

Section 2.0:
MODIFICATIONS TO STAGSUNIT (the program called "stagun.src")

Items 796 and 797 in the long file, ...panda2/doc/panda2.news, document the modifications to the PANDA2 processor, STAGSUNIT. These two new items of panda2.news are reproduced below.

Section 2.1:
Item No. 796 in the File, ...panda2/doc/panda2.news
----
796. October, 2009
The STAGSUNIT processor, stagun.src, was modified. STAGSUNIT is a PANDA2
processor that, given some input data from the user, automatically
generates valid input files, *.bin and *.inp, for STAGS. A new input datum
was added at the end of the interactive STAGSUNIT session, which generates
the *.STG file (input for STAGSUNIT). An example of a new *.STG file for a
case (an axially compressed, axially stiffened panel) called "allen2"
follows:

```
      n           $ Do you want a tutorial session and tutorial output?
        1         $ Choose type of STAGS analysis (1,3,4,5,6),INDIC
        0         $ Restart from ISTARTth load step (0=1st nonlinear soln), ISTART
  1.000000        $ Local buckling load factor from PANDA2, EIGLOC
      y           $ Are the dimensions in this case in inches?
        0         $ Nonlinear (0) or linear (1) kinematic relations?, ILIN
        0         $ Type 1 for closed (360-deg) cyl. shell, 0 otherwise, ITOTAL
 13.00000         $ X-direction length of the STAGS model of the panel: XSTAGS
 55.00000         $ Panel length in the plane of the screen, L2
      y           $ Is the nodal point spacing uniform along the stringer axis?
       51         $ Number of nodes in the X-direction: NODEX
 -100.0000        $ Resultant (e.g. lb/in) normal to the plane of screen, Nx
        0         $ Resultant (e.g. lb/in) in the plane of the screen,    Ny
        0         $ In-plane shear in load set A,                        Nxy
        0         $ Normal pressure in STAGS model in Load Set A, p
        0         $ Resultant (e.g. lb/in) normal to the plane of screen, Nx0
        0         $ Resultant (e.g. lb/in) in the plane of the screen,    Ny0
        0         $ Normal pressure in STAGS model in Load Set B, p0
  1.000000        $ Starting load factor for Load System A, STLD(1)
        0         $ Load factor increment for Load System A, STEP(1)
  1.000000        $ Maximum load factor for Load System A, FACM(1)
        0         $ Starting load factor for Load System B, STLD(2)
        0         $ Load factor increment for Load System B, STEP(2)
        0         $ Maximum load factor for Load System B, FACM(2)
        1         $ How many eigenvalues do you want? NEIGS
      480         $ Choose element type: 410 or 411 or 480 or 940
      n           $ Have you obtained buckling modes from STAGS for this case?
       57         $ Number of stringers in STAGS model of 360-deg. cylinder
        0         $ Number of rings in the STAGS model of the panel
      n           $ Are there rings at the ends of the panel?
        5         $ Number of finite elements between adjacent stringers
       13         $ Number of finite elements between adjacent rings
        3         $ Stringer model: 1 or 2 or 3 or 4 or 5(Type H(elp))
        3         $ Ring model: 1 or 2 or 3 or 4 or 5 (Type H(elp))
        0         $ Reference surface of cyl: 1=outer, 0=middle, -1=inner
      n           $ Do you want to use fasteners (they are like rigid links)?
      n           $ Are the stringers to be "smeared out"?
      n           $ Are the rings to be "smeared out"?
```

```
        5          $ Number of nodes over height of stiffener webs, NODWEB
        5          $ Number of nodes over width of stringer flange, NDFLGS
        5          $ Number of nodes over width of ring flange, NDFLGR
     n             $ Do you want stringer(s) with a high nodal point density?
     n             $ Do you want ring(s) with a high nodal point density?
     n             $ Is there plasticity in this STAGS model?
     n             $ Do you want to use the "least-squares" model for torque?
     n             $ Is stiffener sidesway permitted at the panel edges?
     n             $ Do you want symmetry conditions along the straight edges?
        1          $ Edges normal to screen (0) in-plane deformable; (1) rigid
new-->  1          $ Edges parallel to screen (0) in-plane deformable; (1) rigid
----------------------------------------------------------------------
```

The last line in the allen2.STG file is the new input datum for STAGSUNIT.
In this case (allen2) the axial displacement, u, is forced to vary
linearly across the width of the two axially loaded edges of the panel: at
the top (x=0) and at the bottom (x=XSTAGS) of the portion of the panel
being analyzed by STAGS. The width-wise linear variation of axial
displacement u is enforced by 2 x (ncols(1)-2) additional Lagrange
constraint equations, in which ncols(1) is the number of columns in Shell
Unit 1 of the STAGS model of the panel. (Shell Unit 1 is the panel skin.)

The STAGSUNIT user is prompted for the new input datum via a new entry in
the .../panda2/execute/PROMPT.DAT file, as follows:
```
----------------------------------------------------------------------
400.1 Edges parallel to screen (0) in-plane deformable; (1) rigid
400.2
      This input is for the STAGS model of the panel generated via
      the command "STAGSUNIT".

      Choose 0 if you think the two edges of the panel that run
      parallel to the rings (panel width-wise coordinate direction
      or circumferential direction) ARE relatively free to deform
      in the x-direction, that is, in the axial direction in the
      plane of the panel skin.

      Choose 1 if you think these two edges of the panel ARE NOT
      free to deform in the x-direction.

      NOTE:  The projection of these two edges onto the surface of
             the undeformed panel are ALWAYS free to move in the
             x-direction as straight lines.
----------------------------------------------------------------------
```
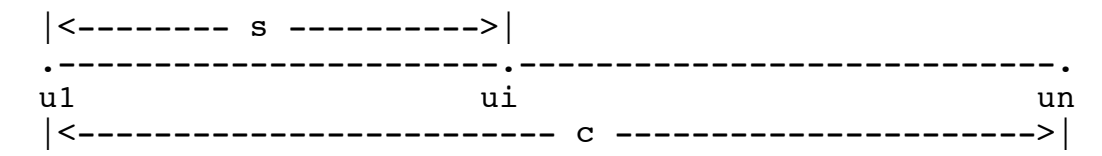
Here is how the linear variation of axial displacement u is imposed along
the two axially loaded edges in the STAGS model. Only Unit 1 in the STAGS
model is involved in the "linear-u" constraint conditions. The sketch
below shows a schematic of one of the two axially loaded edges of the

STAGS model of the panel.

```
  |<-------- s ---------->|
  .----------------------.--------------------------.
  u1                      ui                         un
  |<--------------------- c --------------------->|
```

"c" is the width of the panel and "s" is the distance from where column 1
is located to where column i is located in the STAGS model. For the
axially loaded edge at the beginning of the STAGS model (row 1), u1 is the
axial displacement (normal to the screen) at row 1, column 1. ui is the
axial displacement at row 1, column i. un is the axial displacement at row
1, column n. For the axially loaded edge at the end of the STAGS model
(row m) the locations are the same except that "row 1" is replaced by "row
m", in which m denotes the last row in Unit 1 of the STAGS model. If the
axial displacement u is to vary linearly over the entire width of the
panel along each of these two axially loaded edges, we must have at each
edge:

  ui = u1(1 - s/c) + un(s/c)   (796.1)

The constraint condition in STAGS must be of the form:

  sum-over-i[ai*ui] + ao = 0   (796.2)

In our case a0 = 0, and we have the following three terms in the
constraint equation (796.2) to be multiplied by a Lagrange multiplier:

  a1 = (s/c - 1);   a2 = 1.0;   a3 = -s/c   (796.3)

in which a2 is the coefficient of the term, ui, in Eq.(796.2). and a3 is
the coefficient of the term, un, in Eq.(796.2). The STAGS user's manual
recommends that a scale factor such as the panel skin axial stiffness,
CX(1,1,1) = STIFF, be used in the Lagrange constraints. Therefore, in the
following new FORTRAN coding listed below, we have CC1 = STIFF x a1, CC2 =
STIFF x a2, CC3 = STIFF x a3.

There are n-2 Lagrange constraints for each of the two axially loaded
edges, in which n is the number of columns in Shell Unit 1 of the STAGS
model. Each of these Lagrange constraint conditions has three terms, with
coefficients, CC1, CC2, and CC3.

The STAGSUNIT processor, stagun.src, was modified as follows:

(lines skipped to save space. See Item No. 796 in the file,
 ...panda2/doc/panda2.news)

The new input datum permits comparisons of local postbuckling behavior of axially compressed, axially stiffened curved and flat panels in which in-plane warping is permitted (IEDGE2 = 0) and prevented (IEDGE2 = 1). This comparison is permitted only for STAGS models of panels previously analyzed or optimized by PANDA2. There is only a single model for local postbuckling behavior incorporated into PANDA2, that described in detail in the paper:

Bushnell, D., "Optimization of composite, stiffened, imperfect panels under combined loads for service in the postbuckling regime", Computer Methods in Applied Mechanics and Engineering, Vol. 103 (1993) 43-114

Therefore, this new panda2.news item does not affect optimum designs obtained with PANDA2. It only affects the EVALUATION of these designs obtained through the execution of STAGS in which the input data for STAGS are generated via the PANDA2 processor, STAGSUNIT.

******************** END OF SUB-SECTION 2.1 ****************************

Section 2.2:
Item No. 797 in the File, ...panda2/doc/panda2.news
----
797. November, 2009
The STAGSUNIT processor, stagun.src, was modified again. This modification has to do with the behavior of a STAGS model of a panel previously optimized by PANDA2 in which local postbuckling of the panel skin is permitted at loads lower than the design load. In other words, the local buckling load factor of safety, FSLOC, is significantly less than zero during optimization by PANDA2.

Previously, in STAGS models of the local postbuckling behavior of axially compressed panels and shells previously designed by PANDA2, there occurred significant overall axial bending of the panel for applied loading exceeding that at which local skin buckling occurred. The amplitude of this overall axial bending increased as the applied loading increased above the local panel skin buckling load. This overall axial bending of locally postbuckled panels is not included in the PANDA2 model. The overall axial bending is caused by a shift in the location of the neutral axis as the average axial stiffness (C11) of the locally postbuckled panel skin decreases to about half of its unbuckled value.

A new control index called IBCX0XL has been introduced into the input data called for during the interactive STAGSUNIT session. The role of this new

control index is described in the modified PROMPT.DAT file, as follows:

404.0
     Next, you will be asked to provide an index, IBCX0XL, which
     controls the distribution of axial displacement u over the
     heights of the webs of the stringers at axial stations x=0
     and x=XSTAGS, which are the axial coordinates at the two
     axially loaded ends of the STAGS model of the panel.
     The index, IBCX0XL, is defined as follows:

     IBCX0XL=0: no constraint of u is imposed over each stringer
               web height in the STAGS model of the panel.

     IBCX0XL=1: u=constant is imposed over the height of each
               stringer web in the STAGS model of the panel.

     There is the following reason for the introduction of the
     index, IBCX0XL: The panel is designed to buckle locally at
     a load less than the design load, that is, the factor of
     safety for local buckling, FSLOC, is less than 0.9. We
     wish to simulate in the STAGS model the same end conditions
     that exist in the PANDA2 model for the precollapsed state
     of the locally postbuckled panel. By forcing the axial
     displacement u to be constant over the heights of the
     stringer webs, we prevent the overall axial bending of the
     stringer-stiffened panel that occurs because of the shift
     in the neutral axis caused by the axial softening of the
     panel skin as it deforms in its locally postbuckled state.

     If you have a panel loaded reasonably far into its locally
     postbuckled state at the design load, say FSLOC is less
     than about 0.7, and if the applied load is equal to the
     design load, and if the STAGS model represents a sub-domain
     of the panel analyzed or optimized by PANDA2 (that is,
     XSTAGS is less than the axial length of the panel optimized
     by PANDA2), then you should probably set IBCXOXL = 1 .
     Otherwise, set IBCX0XL = 0 .

405.1 Stringer web axial displacement index, IBCX0XL=0 or 1
405.2
     IBCX0XL=0: no constraint of u over each stringer web height
               in the STAGS model of the panel.

     IBCX0XL=1: u=constant over the height of each stringer web
               in the STAGS model of the panel.

     If you have a panel loaded reasonably far into its locally
     postbuckled state at the design load, say FSLOC is less

than about 0.7, and if the applied load is equal to the
        design load, and if the STAGS model represents a sub-domain
        of the panel analyzed or optimized by PANDA2 (XSTAGS is
        less than the axial length of the panel optimized by
        PANDA2), then you should probably set IBCXOXL = 1 .
        Otherwise, set IBCX0XL = 0 .

An example of the new *.STG file (input data for STAGSUNIT) follows
(allenrng3 case):
----
      n $ Do you want a tutorial session and tutorial output?
        1         $ Choose type of STAGS analysis (1,3,4,5,6),INDIC
        0         $ Restart from ISTARTth load step (0=1st nonlinear soln), ISTART
  1.000000 $ Local buckling load factor from PANDA2, EIGLOC
      y $ Are the dimensions in this case in inches?
        0         $ Nonlinear (0) or linear (1) kinematic relations?, ILIN
        0         $ Type 1 for closed (360-deg) cyl. shell, 0 otherwise, ITOTAL
  9.779300 $ X-direction length of the STAGS model of the panel: XSTAGS
  12.35250 $ Panel length in the plane of the screen, L2
      y $ Is the nodal point spacing uniform along the stringer axis?
       61         $ Number of nodes in the X-direction: NODEX
 -100.0000 $ Resultant (e.g. lb/in) normal to the plane of screen, Nx
        0         $ Resultant (e.g. lb/in) in the plane of the screen,   Ny
        0         $ In-plane shear in load set A,   Nxy
        0         $ Normal pressure in STAGS model in Load Set A, p
        0         $ Resultant (e.g. lb/in) normal to the plane of screen, Nx0
        0         $ Resultant (e.g. lb/in) in the plane of the screen,   Ny0
        0         $ Normal pressure in STAGS model in Load Set B, p0
  1.000000 $ Starting load factor for Load System A, STLD(1)
        0         $ Load factor increment for Load System A, STEP(1)
  1.000000 $ Maximum load factor for Load System A, FACM(1)
        0         $ Starting load factor for Load System B, STLD(2)
        0         $ Load factor increment for Load System B, STEP(2)
        0         $ Maximum load factor for Load System B, FACM(2)
        1         $ How many eigenvalues do you want? NEIGS
      480         $ Choose element type: 410 or 411 or 480 or 940
      n $ Have you obtained buckling modes from STAGS for this case?
      132         $ Number of stringers in STAGS model of 360-deg. cylinder
        2         $ Number of rings in the STAGS model of the panel
      y $ Are there rings at the ends of the panel?
        0         $ Number of finite elements between adjacent stringers
       50         $ Number of finite elements over circumference, NELCIR
       30         $ Number of finite elements between adjacent rings
        3         $ Stringer model: 1 or 2 or 3 or 4 or 5(Type H(elp))
        3         $ Ring model: 1 or 2 or 3 or 4 or 5 (Type H(elp))
        0         $ Reference surface of cyl: 1=outer, 0=middle, -1=inner
      n $ Do you want to use fasteners (they are like rigid links)?
      n $ Are the stringers to be "smeared out"?
      n $ Is the nodal point spacing uniform around the circumference?
  5.095772 $ Circ. callout Y(i) where the nodal point spacing changes, Y(1)

```
      19         $ Number of nodes n(i) from Y(i-1) to Y(i) (n=odd!), n( 1)
       y         $ Are there any more interior axial stations y where dy changes?
  6.228166       $ Circ. callout Y(i) where the nodal point spacing changes, Y( 2)
         9       $ Number of nodes n(i) from Y(i-1) to Y(i) (n=odd!), n( 2)
       y         $ Are there any more interior axial stations y where dy changes?
  7.926756       $ Circ. callout Y(i) where the nodal point spacing changes, Y( 3)
         7       $ Number of nodes n(i) from Y(i-1) to Y(i) (n=odd!), n( 3)
       y         $ Are there any more interior axial stations y where dy changes?
  9.059150       $ Circ. callout Y(i) where the nodal point spacing changes, Y( 4)
         9       $ Number of nodes n(i) from Y(i-1) to Y(i) (n=odd!), n( 4)
       n         $ Are there any more interior axial stations y where dy changes?
      19         $ Number of nodes n(i) from last Y to y = YSTAGS, n( 5)
       n         $ Are the rings to be "smeared out"?
         5       $ Number of nodes over height of stiffener webs, NODWEB
         5       $ Number of nodes over width of stringer flange, NDFLGS
         5       $ Number of nodes over width of ring flange, NDFLGR
       n         $ Do you want stringer(s) with a high nodal point density?
       n         $ Do you want ring(s) with a high nodal point density?
       n         $ Is there plasticity in this STAGS model?
       n         $ Do you want to use the "least-squares" model for torque?
       n         $ Is stiffener sidesway permitted at the panel edges?
       n         $ Do you want symmetry conditions along the straight edges?
         1       $ Edges normal to screen (0) in-plane deformable; (1) rigid
see 796->1       $ Edges parallel to screen (0) in-plane deformable; (1) rigid
new --> 1        $ Stringer web axial displacement index, IBCX0XL=0 or 1
----------------------------------------------------------------------
```

In order to incorporate the modification it is necessary to introduce new
partial compatibility constraints into the STAGS model. Accordingly, The
STAGSUNIT processor, stagun.src, was modified as follows:
```
----------------------------------------------------------------------
(lines skipped to save space. See Item No. 797 in the file,
 ...panda2/doc/panda2.news)
----------------------------------------------------------------------
```
A difficulty introduced by this modification is that the linear bifurcation
buckling load factors will be changed from their former values if IBCX0XL = 1.
With IBCX0XL = 1 these linear buckling load factors may no longer agree well
with PANDA2 predictions, which are based on simple support along the two
axially loaded edges. That is why it is recommended that IBCX0XL be set equal
to unity ONLY for cases in which local postbuckling of the panel skin is an
important ingredient of the behavior of the panel.
********************* END OF SUB-SECTION 2.2 ************************
************************* END OF SECTION 2.0 ************************

Section 3.0:
STAGS PREDICTIONS OF LOCAL BUCKLING AND POST-BUCKLING BEHAVIOR

The remaining figures and tables in this report pertain to this section. **All of the STAGS models include only**

one ring bay of the cylindrical shell optimized by PANDA2. In most of these "one-ring-bay" STAGS models only five stringer bays are included. In all of the STAGS models except two the rings are included at the top and bottom (axial coordinates, x = 0 and x = 9.7793 inches in the "one-ring-bay" models).

*********************** IMPORTANT NOTE ***************************
Stiffeners at the edges of the STAGS models have half the stiffness of those in the interior. This is done so that a relatively small piece (sub-domain) of a large stiffened shell structure will have the same prebuckling load distribution as if that relatively small piece were embedded in the larger whole, and as if symmetry or antisymmetry conditions exist along the edges of the sub-domain included in the STAGS model.
****

There are four STAGS models with one ring bay and only two stringer bays. Two of these include the stiffeners along the edges of the STAGS model. The other two omit the edge stiffeners. These "other two" models simulate certain tests of local buckling and post-buckling of relatively small specimens being conducted at NASA.

In all of the STAGS models the stiffeners are modeled as flexible "shell" branches (Shell Units in STAGS jargon). All of the STAGS models, except the two models: "one-ring-bay, two-stringer-bays without edge stiffeners", are generated with use of the PANDA2 processor called "STAGSUNIT". The "one-ring-bay, two-stringer-bays without edge stiffeners" models are generated starting with the "one-ring-bay, two-stringer-bays with edge stiffeners" model and suitably editing the *.inp file essentially to eliminate the effect of the edge stiffeners by changing their dimensions and material properties (making them very tiny and very weak).

Section 3.1:
Curved panel with overall axial bending permitted, No edge warping

The case with the name "allenrngs" is discussed in this sub-section.

Figures 21 - 41 and Table 24 pertain to this sub-section. The STAGS cases are called "allenrngs". One ring bay (with edge rings included) and five stringer bays are included in the STAGS model of the curved shell, which was previously optimized by PANDA2.

Table 24 presents details of the run stream used to generate the STAGS results for this case. Included in Table 24 are some comments and discussion to explain what is going on. The reader should be able to use Table 24 (and Table 25 for the flat panel) as a sort of user's manual on how to generate STAGS results for cases that may be rather difficult because of the possible presence of mode jumping.

Figure 21 shows the linear bifurcation buckling mode shape and eigenvalue, pcr = 3.3679. There is reasonably good agreement with PANDA2, which obtains a local buckling load factor of 3.1363 corresponding to an applied load, Nx = -100 lb/in. PANDA2 predicts that the critical (lowest) local buckling load is associated with a mode shape that has six halfwaves over the distance between adjacent rings (optimized ring spacing = 9.7793 inches). In the PANDA2 model of local buckling the rings are replaced by simple support boundary conditions. The STAGS prediction in Fig. 21 indicates that the edges at x = 0 and x = 9.7793 inches are more like clamped edges than simply supported edges. This difference probably explains why the STAGS eigenvalue, 3.367878, is somewhat higher than that predicted by PANDA2 for Nx = -100 lb/in: 3.1363 for local buckling between rings.

On page 3 of Table 24 are given some of the STAGS results for the first nonlinear static (INDIC=3) run. In this "allenrngs" case nonlinear static convergence succeeded throughout the load range up to and including the design load, PA = 10.0 (Nx = -1000 lb/in). Figures 22 and 23 pertain to the STAGS model called "allenrngs" in which a uniform finite element mesh is used. Pages 4 - 8 of Table 24 pertain to the STAGS model generated with the use of Table 12 instead of Table 14, but with the new overall axial bending index, IBCX0XL = 0 instead of IBCX0XL = 1, as is listed in Table 12. Results from this new STAGS model are displayed in Figs. 24 and 25. Note that finite elements are concentrated in the neighborhood of stringer no. 3, counting stringers from the bottom right-hand edge of the STAGS model.

In comparing Figs. 23 and 24 we see that in order to obtain reasonably well converged values for the maximum effective stresses in the panel skin we need a very refined finite element mesh in the neighborhood of at least one of the central stringers. In comparing Fig. 24 with Fig. 25 we see that the maximum effective stress in the curved panel occurs in the panel skin at the outer fiber. The outer fiber is on the panel skin surface opposite from that to which the internal stringers are attached.

The maximum outer fiber effective stress, 85330 psi (Fig. 24), is much higher than the maximum effective stress predicted by the PANDA2 model: **sbar = 56068 psi** which appears among the data listed under Comment no. 7 in sub-sub-section 1.1.2. The large difference between 85330 psi and 56068 psi is caused by the following:

1. For the curved panel STAGS predicts significantly larger maximum inward local post-buckling displacement than maximum outward local post-buckling displacement. This difference in maximum inward and outward displacement cannot be reproduced by the simple "flat" model used by PANDA2 [3,22], which is based on the single, flat, discretized module model shown in Figs. 5 - 7.

2. The simple model used in PANDA2 cannot predict the overall axial bending of the panel displayed in Figs. 28 and 29.

3. In the simple PANDA2 model the deformations of the cross section of the single discretized module model resemble the local buckling mode, with limited modification ("flattening") of this mode as the load reaches the far-local-post-buckling regime. See Refs.[3,22] for details of the local post-buckling theory used in PANDA2.

Note that the maximum effective stress always occurs in the panel skin, not in any of the stiffeners.

In the panel skin of the STAGS model of the curved panel the "outer" fiber is the fiber on the opposite surface of the panel skin from that containing the root of the internal stringer. The maximum effective stress occurs on the surface of the panel skin opposite from the surface of the panel skin to which the stringer is attached. For the flat panel the maximum effective stresses on both panel skin surfaces ("outer" and "inner" surfaces in Figs. 54 and 55) are approximately the same. This difference in behavior with regard to the curved and the flat panel occurs because in the curved panel the maximum inward local post-buckling displacement significantly exceeds the maximum outward local postbuckling displacement (Fig. 26) and because the maximum effective stress occurs at locations with large positive hoop stress combined with significant negative axial stress, as is the situation in the expanded regions displayed in Fig. 24 for the curved panel with overall axial bending and in Fig. 54 for the flat panel without overall axial bending. As we shall see later the local post-buckling behavior of the STAGS model of the flat panel more closely approximates the post-buckling predictions from PANDA2.

If in Fig. 22 the reader holds a straight edge connecting the two ends of the intersection of either one of the central stringers with the panel skin (either Stringer no. 3 or Stringer no. 4, counting from the lower right-hand edge of the panel, one sees that there is significant overall inward axial bending of the panel depicted in Fig. 22. The overall inward axial bending occurs because the new index, IBCX0Xl, is set equal to zero in the allenrngs.STG file. See Table 14 and the discussion in Sub-Section 2.2.

Figure 26 shows inner and outer normal displacements near the panel center. For the curved panel the depths of the inward buckles far exceed those of the outward buckles. With overall axial bending permitted the depth of the inward buckles is far greater than that predicted by PANDA2 (Fig. 4). PANDA2 predicts the same buckle depth for both inward and outward buckles, since in the PANDA2 local post-buckling theory [3,22] the normal displacement w of the panel skin is assumed to vary sinusoidally in the axial coordinate direction.

Figure 27 shows load-end-shortening curves from PANDA2 and STAGS. The STAGS curve exhibits greater end shortening because there is significant overall axial bending that increases nonlinearly as the applied axial compression Nx exceeds the initial local buckling load, Nx = -313.75 lb/in (PA = 3.1375). This overall axial bending does not occur in the PANDA2 model of local post-buckling behavior [3,22], which is based on an approximate theory in which the locally postbuckled panel has the single module cross section deformation shown in Figs. 5 and 7 with sinusoidal variation in the axial direction. One full axial wavelength of the local post-buckling deformaion as predicted by PANDA2 is displayed in Fig. 7.

The load-end-shortening curve from PANDA2 shown in Fig. 27 is obtained from the axial strain versus Nx curve in Fig. 8: the end shortening between rings at each load step is computed by multiplying the axial strain at that load step by the ring spacing, 9.7793 inches.

Figure 28 demonstrates why the load-end-shortening curve from STAGS exhibits greater abscissa values than the curve from PANDA2 for loads exceeding the local buckling load. In Fig. 28 the axial displaement u that represents one end shortening value plotted in Fig. 27 (the value of u from STAGS at load factor, PA = 10.0) is u at the lower left-hand corner of the stringer shown in Fig. 28. That point in Fig. 28 is at the axial coordinate, x = 0 where the panel skin is attached to the stringer. The value of u at that point is greater than at any other point in the panel cross section at axial coordinate, x = 0.

Figures 28 and 29 show how one of the central stringers in Fig. 22 bends in its plane when the axial displacement u is allowed to vary over the heights of the stringer webs at the ends, x = 0 and x = 9.7793 inches, of the one-ring-bay panel. In the STAGS case called "allenrngs", overall axial bending of the panel is permitted because the new index, IBCX0XL, equals 0 in the allenrngs.STG file. (See Table 14 and Sub-Section 2.2). Execution of STAGSUNIT with use of the allenrngs.STG file listed in Table 14 as input produces the allenrngs.bin and allenrngs.inp files as input files for STAGS. In the view of the third stringer shown in Figs. 28 and 29 the panel skin is attached at the lower edge of the stringer. The panel bends upward in the post-local-buckling regime in this particular view (which corresponds to radially inward axial bending of the internally stiffened, five-stringer-bay panel displayed in Figs. 22, 24 and 25) because the applied axial load distribution at axial stations x = 0 and at x = 9.7793 inches in the panel skin and in the stringers remains fixed during the loading but the skin becomes less stiff in its locally postbuckled state than in its undeformed state. Therefore, the neutral axis of the locally post-buckled panel has shifted upward while the applied axial load distribution at x = 0 and x = 9.7793 inches has remained the same. This upward shift in the neutral axis in the presence of unchanging applied axial load distribution over the panel skin and stringers at x = 0 and x = 9.7793 inches gives

rise to equal and opposite effective end moments that bend the panel upward in the Fig. 28 view (inward in the Fig. 22 view) increasingly as the applied axial load is increased above the local buckling load, Nx = -313.75 lb/in (PA = 3.1375).

As we shall see in the next sub-section the overall behavior of the panel is quite different when the PANDA2 user sets the new index, IBCX0XL = 1 instead of 0, thereby preventing overall axial bending of the axially compressed panel in the loading regime where the panel has buckled locally.
************************ END OF SUB-SECTION 3.1 *****************************

Section 3.2:
Curved panel with overall axial bending NOT permitted, NO edge warping

Figures 30 - 41 and Tables 7 - 13 pertain to this sub-section.

Figure 30 shows the linear buckling mode. In developing this report the writer explored several different finite element meshes, finally settling on one called "allenrngs34803" as the "best" for application to panels in which significant local post-buckling is allowed to occur at the design load. The STAGS model produced by the PANDA2 processor called STAGSUNIT with input data listed in Table 12 produces the two input files, allenrngs34803.bin and allenrngs34803.inp, for STAGS.

In this model one ring bay and five stringer bays are included in the STAGS model, that is:

```
 9.77930    $ X-direction length of the STAGS model of the panel: XSTAGS
12.35250    $ Panel length in the plane of the screen, L2
```

are used in the *.STG file listed in Table 12. Edge warping and overall axial bending are prevented by the three input lines:

```
  1    $ Edges normal to screen (0) in-plane deformable; (1) rigid
  1    $ Edges parallel to screen (0) in-plane deformable; (1) rigid
  1    $ Stringer web axial displacement index, IBCX0XL=0 or 1
```

at the end of the *.STG file listed in Table 12. Variable nodal point spacing in the circumferential coordinate direction is specified in the *.STG file listed in Table 12 by the lines:

```
   n        $ Is the nodal point spacing uniform around the circumference?
5.095772  $ Circ. callout Y(i) where the nodal point spacing changes, Y( 1)
     19   $ Number of nodes n(i) from Y(i-1) to Y(i) (n=odd!), n( 1)
   y        $ Are there any more interior axial stations y where dy changes?
5.378870  $ Circ. callout Y(i) where the nodal point spacing changes, Y( 2)
      3   $ Number of nodes n(i) from Y(i-1) to Y(i) (n=odd!), n( 2)
   y        $ Are there any more interior axial stations y where dy changes?
5.945067  $ Circ. callout Y(i) where the nodal point spacing changes, Y( 3)
     17   $ Number of nodes n(i) from Y(i-1) to Y(i) (n=odd!), n( 3)
   y        $ Are there any more interior axial stations y where dy changes?
6.228166  $ Circ. callout Y(i) where the nodal point spacing changes, Y( 4)
      3   $ Number of nodes n(i) from Y(i-1) to Y(i) (n=odd!), n( 4)
```

```
      y        $ Are there any more interior axial stations y where dy changes?
7.926756       $ Circ. callout Y(i) where the nodal point spacing changes, Y( 5)
       7       $ Number of nodes n(i) from Y(i-1) to Y(i) (n=odd!), n( 5)
      y        $ Are there any more interior axial stations y where dy changes?
9.059150       $ Circ. callout Y(i) where the nodal point spacing changes, Y( 6)
       9       $ Number of nodes n(i) from Y(i-1) to Y(i) (n=odd!), n( 6)
      n        $ Are there any more interior axial stations y where dy changes?
      19       $ Number of nodes n(i) from last Y to y = YSTAGS, n( 7)
```

Note that for a curved (cylindrical) panel the quantities, Y(i), just listed are in degrees, not arc length.
(Y(i) are lengths in the case of a flat panel.) Variable nodal spacing in the circumferential direction is used to
provide enough refinement in the panel skin under one of the central stringers (Stringer no. 3, counting from the
lower right-hand edge of the STAGS model in Fig. 22) in order to obtain reasonably well converged values of
the extreme fiber maximum effective stress in the locally post-buckled panel as loaded by the design load. Only
one ring bay need be included in the STAGS model in order to determine the local post-buckling behavior with
sufficient accuracy. However, it is felt that at least five stringer bays should be included in the STAGS model in
order to eliminate spurious edge effects propagating inward from the two straight panel edges (generators of the
cylindrical panel). After all, the main purpose of using STAGS in this exercise is to evaluate the quality of the
predictions from the PANDA2 analysis of a panel that was previously optimized by PANDA2 for a complete,
internally stiffened cylindrical shell. We do not want to have to model the entire cylindrical shell with STAGS
in order to determine the very local post-buckling behavior, but we want to include enough of the cylindrical
shell to avoid the introduction of edge effects that are not present in the complete cylindrical shell.

Figure 31 shows the deformed state of the panel at the design load, PA = 10.0 (Nx = -1000 lb/in). Compare Fig.
31 with Fig. 22, which corresponds to the "allenrngs" case for which overall axial bending is permitted
(IBCX0XL = 0 in the *.STG file). Note that the maximum inward buckle depth, -0.05733 inch, in Fig. 31 is
significantly less than that in Fig. 22 for the case in which overall axial bending is permitted.

Figure 32 shows an end view of the same deflection pattern as that in Fig. 31. Figure 33 gives a comparison of
the depths of the inward and outward buckles for the IBCX0XL = 0 (overall axial bending permitted) and the
IBCX0XL = 1 (overall axial bending NOT permitted) STAGS models. In Fig. 34 predictions from PANDA2
and STAGS are compared. **In the PANDA2 post-local-buckling model overall axial bending is never
permitted because the post-buckled state is computed with the assumption that the panel is infinitely long
and the variation of normal displacement in the axial coordinate direction is sinusoidal [3,22].**

Figure 35 shows load-end-shortening curves from PANDA2 and from the two STAGS models, one generated
with IBCX0XL = 0 (overall axial bending permitted) and the other generated with IBCX0XL = 1 (overall axial
bending not permitted). Better agreement between the PANDA2 trace and the second STAGS trace in Fig. 35
was expected because the two curves lay atop one another for the optimized design developed before the bug
was discovered in SUBROUTINE MODE. (See Item No. 804 in …panda2/doc/panda2.news.) Figures a1 and
a2 in the appendix show the predictions from STAGS of the distributions of outer fiber (Fig. a1) and inner fiber
(Fig. a2) axial strain in the panel skin of the flat panel at the design load, PA = 10.0 (Nx = -1000 lb/in). The end
shortening of the panel skin at x = 0 at the web root of the third stringer, counting stringers from the bottom
right-hand edge of the STAGS model, is 0.023172 inches at PA = 10.0. This implies an average axial strain
along that "generator" of 0.023172/9.7793 = 0.0023694. It seems to the writer that the average axial strains that
could be derived along that generator from the expanded inserts in both Figs. a1 and a2 would be greater than
0.0023694. This discrepancy remains a small mystery to the writer.

Figures 36 and 37 show the distributions of the outer and inner fiber effective stress in the panel skin. Note that the maximum outer fiber effective stress is considerably greater than the maximum inner fiber effective stress. The outer fiber is on the panel skin surface opposite from that to which the internal stringers are attached. Compare the maximum outer fiber effective stress, **67660 psi**, with the maximum effective stress predicted by PANDA2, **56068 psi**, which is listed in sub-sub-section 1.1.2 under Comment No. 7.

Figures 38 and 39 are analogous to Figs. 28 and 29 for the panel in which overall axial bending is permitted. In the STAGS model generated via Table 12 overall axial bending is prevented by forcing the axial displacement u to be uniform over the heights of all the stringer webs at both ends of the cylindrical panel.

From Fig. 36 it is seen that the maximum outer fiber effective stress occurs in Finite Element No. 259. Finite Element No. 259 is located eight ranks of finite elements from the curved edge at x = 0 and adjacent to Stringer no. 3 on the right-hand side of Stringer no. 3 as we look along the x-axis. Figure 40 gives a plot of the effective stresses on the Bottom and Top surfaces of the panel skin and at the nine integration points in Finite Element No. 259 versus the axial load factor, PA. The maximum effective stress occurs in the "Top" fiber at the 8th integration point in the finite element. The "Top" fiber is on the panel surface opposite from that to which the internal stringers are attached, that is, the outer surface of the cylindrical shell. Integration Point No. 8 is the integration point closest to the stringer and at the mid-axial-length of the finite element. From Figure 40 we see that at the design load, PA = 10.0, there is a significant variation of effective stress in the outer surface of the cylindrical shell over the area of the rather small finite element 259: In Finite Element No. 259 the maximum outer ("Top") surface effective stress is about 69000 psi (Integration Point 8), and the minimum outer surface effective stress is about 57000 psi (Integration Point 1).

Figure 41 shows the "hoop" (circumferential) change in curvature of the panel skin in the same finite element that contains the maximum outer fiber effective stress. The circumferential change in curvature at the design load, PA = 10.0 (Nx = -1000 lb/in) is equal to approximately **0.465 1/inch**. This STAGS prediction is significantly greater that the PANDA2 prediction of **0.354 1/inch** listed in sub-sub-section 1.1.2 under Comment No. 7. **The greater maximum hoop curvature change obtained from the STAGS model of the curved panel is responsible for the greater prediction of maximum effective stress in the STAGS model.**

*************************** IMPORTANT NOTE ****************************
A much improved design might be developed by including a tapered faying flange at the root of each stringer. This would lead to a less localized concentration of change in hoop curvature in the immediate neighborhood of the root of each stringer. PANDA2 cannot handle tapered flanges.

NOTE: The STAGS model produced by STAGSUNIT does not model a stringer faying flange in a rigorous enough manner properly to predict what the actual localized hoop curvature change would be when the stringer faying flange actually bends over its width, as would be the case if the stringer faying flange is either bonded to the stringer base over the entire width, B2(STR), of the stringer base or if the stringer faying flange actually forms an integrated part of the total thickness of Segment No. 2 of the skin/stringer module. What STAGSUNIT does in the case of a stringer (or ring) faying flange is simply attach the faying flange to only one line-of-intersection, either to the panel skin if the stiffener is not a Z-stiffener or to the stiffener web root if the stiffener is a Z-stiffener. Hence, in the STAGSUNIT formulation the stringer faying flange does not bend in the circumferential direction with the panel skin beneath it. Therefore, it will not serve to help reduce the localized hoop curvature concentration in STAGS models produced by the PANDA2 processor, STAGSUNIT.

Unfortunately, as things presently stand with STAGSUNIT, if Segment No. 2 of the skin/stringer module in the PANDA2 model is thicker than Segment No. 1, and if the user wants a more representative STAGS model than that produced by STAGSUNIT as just described, he or she will have to set up STAGS models independently of STAGSUNIT.
****
******************* END OF SUB-SUB-SECTION 3.2 *********************

Section 3.3:
Curved panel with overall axial bending NOT permitted, YES edge warping

The case is called "allenrngs4". Figures 42 - 45 pertain to this sub-section. The STAGS model is generated by STAGSUNIT with the input listed in Table 12 except that the final three lines of the allenrngs4.STG file now read as follows:

```
   0     $ Edges normal to screen (0) in-plane deformable; (1) rigid
   0     $ Edges parallel to screen (0) in-plane deformable; (1) rigid
   1     $ Stringer web axial displacement index, IBCX0XL=0 or 1
```

All four edges of the panel skin are free to undergo in-plane warping, but overall axial bending is prevented. (See Sub-section 2.2 for information on IBCX0XL.)

Figure 42 shows the distribution of outer fiber effective stress at the design load. The maximum value, 81920 psi, is rather high. As is demonstrated in Fig. 42, this maximum effective stress occurs near the edge at x = 9.7793 inches where there is an interaction between the edge warping of the panel skin and the very local stress concentration adjacent to the stringer.

Figure 43 gives plots of end shortening versus axial load factor PA from PANDA2 (trace 1) and from STAGS at 11 nodal points along the axially loaded edge at x = 0. The PANDA2 trace in Fig. 43 is the same PANDA2 curve as those in Figs. 27 and 35. The STAGS load-end-shortening curves are different from each other because there is in-plane edge warping along the axially loaded panel end at x = 0. Six of the nodes used for the STAGS plots (Nodes 1, 11, 29, 49, 61, and 71) correspond to points on the panel skin reference surface where the internal stringers are attached. The remaining five nodes correspond to points on the panel skin at x = 0 midway between adjacent stringers.

Figures 44 and 45 show the circumferential displacements at three axial stations, x = 0, x = L/2, and x = L (L = 9.7793 inches) on each of the two straight edges, y = 0 (Fig.44) and y = 12.3525 inches. (Fig.45)
********************* END OF SUB-SECTION 3.3 *********************

Section 3.4
Flat panels with overall axial bending NOT permitted, NO edge warping

Figures 46 - 66 and Tables 15 - 23 and Table 25 pertain to this sub-section. Tables 15 - 23 have already been cited above in sub-sub-section 1.2.1 for the 5-stringer-bay flat panel and in sub-sub-section 1.2.2 for the 10-stringer-bay flat panel. The relevant run streams that apply to executions of the PANDA2 processors are also given there.

There is no further optimization relating to the flat panels. In the remainder of this report the skin/stringer panel module cross section, ring spacing, and ring dimensions are the same as those obtained from optimization of the curved panel, as follows:

```
-----------------------------------------------------------------
 DIMENSIONS OF  CURRENT  DESIGN...
VARIABLE CURRENT
 NUMBER   VALUE             DEFINITION
  1     2.4705E+00     B(STR):stiffener spacing, b: STR seg=NA, layer=NA
  2     8.2342E-01    B2(STR):width of stringer base, b2 (must be > 0, see
  3     8.4714E-01     H(STR):height of stiffener (type H for sketch), h: S
  4     2.4141E-02 T(1 )(SKN):thickness for layer index no.(1 ): SKN seg=1
  5     8.0087E-02 T(2 )(STR):thickness for layer index no.(2 ): STR seg=3
  6     9.7793E+00     B(RNG):stiffener spacing, b: RNG seg=NA, layer=NA
  7     0.0000E+00    B2(RNG):width of ring base, b2 (zero is allowed): RNG
  8     8.4714E-01     H(RNG):height of stiffener (type H for sketch), h: R
  9     6.0060E-02 T(3 )(RNG):thickness for layer index no.(3 ): RNG seg=3
-----------------------------------------------------------------
```

The main purpose of exploring STAGS models of flat panels with the dimensions just listed is to compare the STAGS "flat panel" predictions with the PANDA2 model. This is done here because the PANDA2 local post-buckling theory is based on the behavior of a single discretized skin/stringer module of the type displayed in Figs. 5 - 7. In the post-local-buckling analysis [3,22] PANDA2 assumes that this module is flat even for cases in which the stiffened panel or shell is actually curved.

In setting up the flat panel models with PANDA2 we specify that the rings and stringers are EXTERNAL rather than INTERNAL, as was done for the curved panels. Therefore, in the plots of STAGS models the stiffeners appear on the opposite surface of the panel skin than for the curved panels.

The STAGS 480 finite element is used in all the models described in the remainder of this report. Also, in all the models described in the remainder of this report no in-plane edge warping is permitted and no overall axial bending is permitted. The last three lines of the various *.STG files are as follows:

```
 1  $ Edges normal to screen (0) in-plane deformable; (1) rigid
 1  $ Edges parallel to screen (0) in-plane deformable; (1) rigid
 1  $ Stringer web axial displacement index, IBCX0XL=0 or 1
```

Therefore, we are concentrating our attention only on the edge conditions that, for the curved panel, have been recommended as being the best conditions to apply in STAGS models of panels previously optimized by PANDA2 for cases in which there is significant post-local-buckling behavior at the design load.

In STAGS nonlinear runs of the 5-stringer-bay and 10-stringer-bay models it was necessary to use the transient (INDIC=6) option in order to bypass near singularities on the nonlinear static (INDIC=3) equilibrium path.

The STAGS runstream for the 5-bay flat panel is listed in Table 25.

Section 3.4.1:
Flat Panel with 5 Stringer Bays

Figures 46 - 63 and Table 25 pertain to this sub-sub-section.

All the STAGS models of the 5-bay flat panel have the "circumferentially" varying nodal point spacing identified as "yvariablespacing3" in Table 12, which applies to the curved panel. Hence, the flat panel width-wise nodal point spacing is the same as the recommended choice for the curved panel. It is felt that this nodal point spacing, in which finite elements are concentrated in the panel skin near the root of one of the central stringers, will adequately capture the axially periodic bending stress concentrations that develop there as the panel is loaded well into its locally post-buckled state.

Figure 46 shows the linear buckling mode. There appear to be five axial half waves in this mode. However, the end condtions at x = 0 and at x = 9.7793 inches appear to be more like clamping conditions than simple support conditions. The PANDA2 model of local buckling is based on simple support along x = 0 and x = L. PANDA2 predicts local buckling with six axial half waves rather than five. However, note that if one measures the axial half-wave length of the buckle pattern displayed in Fig. 46, one realizes that if the panel skin were simply supported at x = 0 and at x = L, one would be able to fit six axial halfwaves over the axial length, L = 9.7793 inches.

Figure 47 shows the state of the panel at load factor, PA = 7.1955 (Nx = -719.55 lb/in, or 71.955 per cent of the design load, Nx = -1000 lb/in.) This was the highest load factor for which a converged nonlinear static (INDIC=3) solution could be obtained. A transient (INDIC=6) run was then made at an applied load, PA = 1.05 x 7.1955 = 7.555. In the transient run the stiffness matrix damping factor, BETA, was set equal to 3.0E-04 in this case. (See page 3 of Table 25.)

Figure 48 is a plot of the kinetic energy versus time obtained from a file generated via the command issued in the directory in which the STAGS case is being or has been executed:

```
awk –f ke.awk [input filename] > [output filename]
```

or

```
awk –f ke.awk allenflat.out2 > allenflat.plt
```

The allenflat.plt file generated in this way contains three traces:

trace 1: strain energy vs time
trace 2: kinetic energy vs time
trace 3: total energy vs time

In the cases explored in this report the kinetic energy is always very, very small compared to the strain energy and the total energy. Therefore, before plotting, the allenflat.plt file is edited to remove trace 1 and trace 3. A new title is added, the legend is edited, the x,y axes labels are edited, and a Postscript file of the plot is generated from the command (at the writer's facility):

```
/home/progs/bin/plotps.linux < allenflat.plt > allenflat.ps
```

The plot in Fig. 48 appears on the user's computer screen with the command:

gv allenflat.ps

in which "gv" = "ghost view" (ask your system person what that is!
            You should have "ghost view" on your
            desktop station.)

In Fig. 48 it is interesting that for Time < 0.05 seconds the STAGS transient run almost converges to a static state. However, approximately at Time = 0.05 seconds the kinetic energy begins to increase, then soon rises abruptly to a maximum value of about 0.06 in-lb, followed by a long decay to near-zero values at Time = 0.4 seconds. Dynamic mode jumping is occurring during this time.

Figures 49 - 51 show the deformed states of the flat panel during three times in the transient STAGS run: Time = 0.0522 seconds (Fig. 49), Time = 0.0922 seconds (Fig. 50), and Time = 0.389 seconds (Fig. 51). These three "snapshots" of the deformed state of the panel demonstrate that during the transient phase of the STAGS analysis mode jumping is occurring in the central stringer bay: Figure 49 indicates about 5.5 axial halfwaves, Fig. 50 indicates six axial halfwaves, and Fig. 51 indicates 7 axial halfwaves.

Figure 52 shows the deformed state after load-relaxation and continuing static (INDIC=3) loading up to the design load, PA = 1.0 (Nx = -1000 lb/in). All stringer bays except the central stringer bay exhibit 5 axial half waves in the post-buckled deformation pattern, and the central stringer bay exhibits 7 axial half waves. **This kind of nonuniformity across the width of a multi-stringer-bay panel cannot be predicted with PANDA2 because the local post-buckling theory used in PANDA2 [3,22] is based on the behavior of a single panel module of the type shown in Figs. 5 - 7.**

The PANDA2 model of local post-buckling behavior, being based entirely on a single discretized module model such as that shown in Figs. 5 - 7, cannot predict panel skin deformations with differing numbers of axial half waves in adjacent stringer bays. Also, in the PANDA2 model [3,22] the number of axial half waves in the local post-buckling regime varies smoothly, as shown in Fig. 20, because PANDA2 is based on a model in which the axially loaded boundaries of the panel module play no role. In the PANDA2 post-local-buckling formulation the axial half wavelength of the local buckles plays a role but not the number of axial half waves between two boundaries in the x-coordinate domain. Essentially, in the local post-buckling theory used in PANDA2 the panel is assumed to be infinitely long with a sinusoidal variation of normal displacement in the axial direction, one full axial wavelength of which is displayed in Fig. 7. One of the unknowns in the PANDA2 post-local-buckling theory [3] is an axial wavelength parameter "N" which varies smoothly as the axial loading is increased. The other three unknowns are an amplitude, "f", a "flattening" parameter, "a", and a post-buckling nodal line slope, "m". The Newton method is use to solve the system of nonlinear equations for f, a, m, and N (N is the axial wavelength parameter). Output such as that listed under CHAPTER 16 in sub-sub-section 1.1.2 appears when the print index, NPRINT = 2, in the *.OPT file. We have from PANDA2, for example, the following output in the *.OPM file:

```
 ITER.        UNKNOWNS IN THE LOCAL POSTBUCKLING PROBLEM
   NO.     AMPLITUDE    FLATTENING    NODAL LINE   PI**2*n**2/4L**2 AXIAL HALFWAVLNGTH
             f              a         SLOPE,  m          N           OF BUCKLES,(L/n)
    0     6.28412E-02  -2.15159E-01   2.17492E-02    9.28810E-01    1.62988E+00
```

```
   1     5.95259E-02   -2.44126E-01    1.98637E-02    1.13200E+00    1.47638E+00
   2     5.83214E-02   -2.52053E-01    1.93437E-02    1.21452E+00    1.42533E+00
   3     5.81605E-02   -2.52795E-01    1.92756E-02    1.22529E+00    1.41906E+00
   4     5.81580E-02   -2.52805E-01    1.92746E-02    1.22545E+00    1.41897E+00
      CONVERGENCE SUCCESSFUL!
```

Figure 53 shows an end view of the local post-buckling deformations in the flat panel at the design load, PA = 1.0. Note that in the central stringer bay, where there exist seven axial half waves, the amplitude of the buckles is slightly smaller that the amplitudes in the other four stringer bays in which there exist five axial half waves in the deformation pattern. Also, note that, unlike the curved panel (Fig. 32), the inward and outward buckles have approximately the same amplitude. This difference in behavior of the flat and curved panels has a significant effect on the maximum effective stress: The maximum effective stress in the flat panel is significantly less than that in the curved panel, and in the flat panel the maximum effective stress is approximately the same on either surface of the panel skin. In the curved panel, in this particular case that involves internal stringers, the maximum effective stress occurs on the surface of the panel skin opposite from that to which the internal stringers are attached because the inward buckles have significantly greater amplitude than the outward buckles and because the maximum effective stress occurs where hoop tension due to local hoop bending is combined with axial compression.

Figures 54 - 56 show the distributions of outer and inner surface effective stress in the flat panel skin at the design load, PA = 1.0. The highly concentrated nature of the effective stress is similar to that for the curved panel (Figs. 36 and 37), but the maximum effective stress is signficantly higher in the curved panel (Fig. 36) because the inward buckles in the curved panel have greater amplitude than either the inward or outward buckles in the flat panel.

Figure 57 shows the effective stress versus axial load factor PA for Finite Element Number 329 in the flat panel. The location of Finite Element Number 329 is shown in Fig. 56. This finite element lies adjacent to the third stringer (counting from the bottom right-hand edge in Fig. 55) just outside the central stringer bay and 10 elements from the axially loaded edge at x = 0 (lower left-hand edge in Fig. 55). The horizontal array of data points at PA = 7.555 corresponds to the results from the transient STAGS run. The shift in the curves above the data from the transient run relative to those below is caused by the mode jump: the change from five axial halfwaves in the central stringer bay for loads below PA = 7.555 to seven axial halfwaves in the central stringer bay for loads above PA = 7.555. Figure 57 is analogous to Fig. 40, which pertains to the curved panel. (However, recall that for the curved panel no transient (INDIC=6) STAGS run was needed.)

Figure 58 is analogous to Fig. 41. Note that for the flat panel there is reasonably good agreement between the maximum change in "hoop" curvature predicted from **STAGS** (absolute value of **kappa(yy) = 0.38**) and the maximum change in "hoop" curvature predicted by **PANDA2 (WDDPB = 0.351** as listed in sub-sub-section 1.2.1).

Figures 59 - 61 show respectively the extreme fiber axial strain, "hoop" (circumferential) strain, and in-plane shear strain in Finite Element Number 329. These figures should be compared to the PANDA2 predictions in Figs. 17 - 19. Note especially that the maximum hoop strain in Finite Element Number 329 (about 0.0056 in Fig. 60) is somewhat greater than the maximum "hoop" strain predicted by PANDA2 (about 0.005 in Fig. 18). This difference is caused by the fact that STAGS predicts a somewhat higher maximum change in hoop curvature at the design load (kappa(yy) = about 0.38 1/in in Fig. 58) than the PANDA2 prediction listed in sub-

sub-section 1.2.1: WDDPB = 0.351 1/in. The in-plane shear strains predicted by STAGS for finite element no. 329 are very different from those predicted by PANDA2 in Fig. 19. To obtain a better match a different finite element should have been chosen for a STAGS plot because the maximum in-plane shear strain occurs at a different location in the panel skin from that corresponding to the maximum circumferential or axial strains.

Figure 62 shows a comparison of predictions from PANDA2 for flat and curved panels. The maximum inward and outward normal displacements at inward and outward buckles are plotted versus the same load factor, PA, used in STAGS. The quantity, WMDTOT, referred to in the two legends pertaining to the curved panel, is the uniform radially outward Poisson ratio expansion induced by the applied axial compression.

In Fig. 63 PANDA2 and STAGS predictions for the amplitudes of the inward and outward buckles in the flat panel are compared. the four traces with STAGS results correspond to two traces each for the buckle depth in the second stringer bay and the buckle depth in the central (middle) stringer bay. For static loading above the mode jump at PA = 7.555 the PANDA2 and STAGS predictions are in good agreement. There is no mode jumping in the PANDA2 model because, as has been previously mentioned, the axial wavelength of the local buckles in the post-buckling regime varies smoothly, as is plotted in Fig. 20. This smooth variation of axial wavelength in the PANDA2 model follows from the nature of the local post-buckling formulation used in PANDA2 [3,22].

Section 3.4.2:
Flat Panel with ten Stringer Bays

Figures 64 - 66 and Table 23 pertain to this sub-sub-section.

The third stringer from the bottom right-hand edge in Fig. 64 is attached to panel skin that has finite elements concentrated in the neighborhood of the root of that stringer.

Figure 64 shows the linear buckling load factor, pcr = 3.0279, and mode shape. Following the usual procedure, this mode shape is used as an inital imperfection with amplitude, Wimp = 0.001 inch. (The analogous procedure was used in connection with the 5-stringer-bay flat panel, as described in Table 25.) In this ten-stringer-bay model, as with the 5-stringer-bay model, it was necessary to use a transient (INDIC=6) STAGS analysis in order to avoid near singularities on the nonlinear static equilibrium path. This was done (not documented here), and subsequently, with use of load relaxation and continued nonlinear static loading, we managed to obtain the post-buckled equilibrium state at the design load, PA = 10.0 (Nx = -1000 lb/in).

The kinetic energy plot (not included here) exhibits the same characteristics as those displayed for the five-stringer-bay panel in Fig. 48: an initial diminishment of the kinetic energy until Time equal about 0.05 second followed by a resurgence and decay of the kinetic energy for Time greater than 0.05 second and less than about 0.5 second.

Figure 65, which is analogous to Fig 50 for the five-stringer-bay STAGS model, shows the deformation pattern at step 190, which corresponds to Time = 0.0998 seconds. At this time there exist three stringer bays with six axial halfwaves: stringer bays 2, 4, and 6, counting from the lower right-hand edge of the STAGS model. The rest of the stringer bays have five axial halfwaves. Note that the ring at the panel edge at x = 0 (lower left-hand panel edge in Fig. 65) experiences side-sway over much of its length, and the first axial post-buckled half waves

in stringer bays 1 - 7 correspond uniformly to "inward" (negative) normal displacement w instead of alternate inward and outward normal displacement from stringer bay to stringer bay as is displayed in Fig. 49, for example.

Figure 66 shows the deformation pattern at step 448, after completion of the transient STAGS run and after load-relaxation and the continuation of static loading up to the design load, PA = 1.0. Now all the stringer bays except the last have inward (negative) buckles at both ends of each bay, and stringer bays 2, 4, 6, and 8 each have seven axial half waves. The remaining stringer bays still have five axial halfwaves. Both end rings now exhibit significant side-sway over most of their lengths. The side-sway of the end rings is consistent with the uniform negative buckles at both ends of all of the stringer bays except the last stringer bay.

The post-local-buckling behavior of the ten-stringer-bay STAGS model is consistent with the behavior of the five-stringer bay STAGS model displayed in Figs. 50 - 52.
********************* END OF SUB-SECTION 3.4 *********************

Section 3.5
Flat and Curved Panels with 2 Stringer Bays

The remaining figures and tables in this report (Figures 67 - 86 and Tables 26 - 29) pertain to this sub-section.

The purpose here is to evaluate how representative a test specimen would be that only includes two stringer bays. Small test specimens proposed at NASA designed for loading well into the local post-buckling regime typically include the axial length between two adjacent rings and two stringer bays with only one stringer: a stringer that runs down the mid-width of the test specimen. The two axially loaded ends are typically embedded in an elastomer, an end condition similar to clamping, and the two straight edges (cylindrical shell generators in the case of a curved panel) are supported in some kind of a "V-type" structure that simulates simple support. The question arises, "Will a test specimen of this type behave in the post-local- buckling load regime in the same way with regard to local buckling and post-buckling as does a small section of the complete shell or panel that the test specimen represents?"

We attempt to answer this question by running four STAGS models:

1. Flat Panel with 2 Stringer Bays and with stiffeners along the 4 edges
2. Flat Panel with 2 Stringer Bays and with no stiffeners along the 4 edges
3. Curved Panel with 2 Stringer Bays and with stiffeners along the 4 edges
4. Curved Panel with 2 Stringer Bays and with no stiffeners along the 4 edges

In all these models overall axial bending is prevented and there is no in-plane warping of the four edges. The STAGS 480 finite element is used throughout.

As with all PANDA2 models any stiffeners along the edges of a panel to be analyzed by STAGS have half the stiffness of the like interior stiffeners. With flat panels the stiffeners are "external", whereas with curved panels the stiffeners are "internal". The same uniform-density finite element mesh was used to produce all the results presented in this sub-segment.

Section 3.5.1
Flat Panel with 2 Stringer Bays and with stiffeners along the four edges

Figures 67 - 72 and Table 26 pertain to this sub-sub-section.

Figure 67 shows the linear buckling mode and load factor for the flat panel with edge stiffeners. This linear buckling mode is used as an imperfection shape (with amplitude, Wimp = 0.001 inch) in the nonlinear static (INDIC=3) STAGS analysis to follow. Figure 68 shows the deformed state of the panel at the design load, PA = 10.0. No transient STAGS run was required to obtain converged static nonlinear equilibrium solutions for all values of load factor, PA. Figures 69 - 71 display the outer and inner fiber effective stress distributions in the flat panel at the design load, PA = 10.0. Figure 72 shows the extreme fiber stress distribution in the finite element that exhibits the maximum effective stress adjacent to the stringer that runs along the mid-width of the panel, that is, in the panel skin in Finite Element Number 780. The maximum effective stress in Finite Element No. 780 is close to 60000 psi, which is very close to the maximum effective stress in the second stringer bay of the five-stringer-bay STAGS model, as shown in Figs. 55 - 57.

Section 3.5.2
Flat Panel with 2 Stringer Bays and with no stiffeners along the four edges

Figures 73 - 78 and Table 27 pertain to this sub-sub-section.

Figure 73 shows the linear buckling mode and load factor for the flat panel without edge stiffeners. This linear buckling mode is used as an imperfection shape (with amplitude, Wimp = 0.001 inch) in the nonlinear static (INDIC=3) STAGS analysis to follow. Figure 74 shows the deformed state of the panel at the design load, PA = 10.0. No transient STAGS run was required to obtain converged static nonlinear equilibrium solutions for all values of load factor, PA. Figures 75 - 77 display the outer and inner fiber effective stress distributions in the flat panel at the design load, PA = 10.0. Figure 78 shows the extreme fiber stress distribution in the finite element that exhibits the maximum effective stress adjacent to the stringer that runs along the mid-width of the panel, that is, in the panel skin in Finite Element Number 1100. The maximum effective stress in Finite Element No. 1100 is about **74000 psi**, significantly greater than the maximum effective stress of **60000 psi** pertaining to the two-stringer-bay STAGS model of the flat panel with edge stiffeners. The maximum effective stress is greater in the two-stringer-bay flat panel without edge stiffeners especially because the two edge stringers retard rotation about the two longitudinal edges, resulting in a smaller amplitude of the local buckles at the design load, PA = 10.0. (Compare Fig. 74 with Fig. 68.)

Section 3.5.3
Curved Panel with 2 Stringer Bays and with stiffeners along the four edges

Figures 79 - 82 and Table 28 pertain to this sub-sub-section.

Figure 79 shows the linear buckling mode and load factor. This linear buckling mode is used as an imperfection shape (with amplitude, Wimp = 0.001 inch) in the nonlinear static (INDIC=3) STAGS analysis to follow. Figures 80 and 81 show the outer and inner fiber distributions of effective stress. The maximum effective stress

is in the outer fiber (surface opposite to that to which the stringers are attached). This maximum effective stress is significantly larger than that for the flat panel with the stiffeners at the edges (Fig. 69) because the maximum inward buckling displacement of the curved panel is larger than either the inward or the outward buckling displacments of the flat panel with the edge stiffeners. Figure 82 is analogous to Fig. 40. Finite Element No. 421 contains the maximum effective stress plotted in Fig. 80. Comparson of Figs. 80 and 81 with Figs. 36 and 37 for the five-stringer-bay curved panel reveal that the maximum outer fiber effective stress in the two-stringer-bay panel is slightly less than that in the five-stringer-bay panel and that the maximum inner fiber effective stress in the two-stringer-bay panel is slightly more than that in the five-stringer-bay panel.

Section 3.5.4
Curved Panel with 2 Stringer Bays and with no stiffeners along the four edges

Figures 83 - 86 and Table 29 pertain to this sub-sub-section.

Figure 83 shows the linear buckling mode and load factor. This linear buckling mode is used as an imperfection shape (with amplitude, Wimp = 0.001 inch) in the nonlinear static (INDIC=3) STAGS analysis to follow. Figures 84 and 85 show the outer and inner fiber distributions of effective stress. The maximum effective stress is in the outer fiber (surface opposite from that to which the stringer is attached). This maximum effective stress is significantly larger than that for the curved panel with the stiffeners at the edges because the two longitudinal edges, now without stringers, are free to rotate, giving rise to deeper buckles than experienced by the curved 2-stringer-bay panel with the edge stiffeners. Figure 86 plots the extreme fiber effective stress in the finite element (Element No. 381) that contains the maximum effective stress in Fig. 84.

Section 4.0
CONCLUSIONS

1. It appears to the writer that the small (2-bay) test specimens plannned by NASA for experimental local buckling and post buckling analysis represent the local buckling and post-buckling behavior well enough as a guide for the preliminary design of complete cylindrical shells with respect to these local behaviors. The two-bay panels without edge stringers or rings have lower linear local buckling load factors [flat panel pcr=2.22827 (Fig.73), curved panel pcr=2.886 (Fig.83)] than do the local buckling load factors for the two-bay panels with edge stringers and rings [flat panel pcr=3.023 (Fig.67), curved panel pcr=3.394 (Fig.79)]. The maximum effective stress in the two-bay panels without edge stringers or rings are as follows: flat panel sbar(max)=**74000 psi** (Fig.78), curved panel sbar(max)=**81000 psi** (Fig.86), whereas the maximum effective stress in the two-bay panels with edge stringers and rings are as follows: flat panel sbar(max)=**59000 psi** (Fig.72), curved panel sbar(max)=**68000 psi** (Fig.72). Therefore, the proposed test specimens appear to be conservative but not horribly conservative.

2. The five-stringer-bay STAGS models appear to be wide enough so that what goes on in the central stringer bay and its neighboring stringer bays is essentially the same as what goes on in each stringer bay (or in alternate stringer bays) of a complete cylindrical shell. For the flat and curved five-stringer-bay STAGS models the maximum effective stresses in the neighborhood of the third stringer from the longitudinal edge of the panel are as follows: curved panel: sbar(max)=**68000 psi** (Fig.40) (**PANDA2 predicts sbar(max)=56068 psi**) flat panel: sbar(max)=**59000 psi** (Fig.57) (**PANDA2 predicts sbar(max)=53921 psi**).

3. **PANDA2 underpredicts the maximum effective stress in a curved panel in which the design load is about three times the local buckling load.** This underprediction is caused by the inability of the PANDA2 local post-buckling model to generate different post-buckling amplitudes for inward and outward local buckles in the panel skin. This characteristic of PANDA2 results from the fact that the local post-buckling behavior is generated from a single discretized module in which the panel skin is assumed to be flat (Figs. 5-7) and the variation of normal displacement in the axial coordinate direction is assumed to be sinusoidal.

4. Enough information is given in this text so that the reader can reproduce the PANDA2 results at his or her facility. Enough information is given in Tables 24 and 25 so that the reader can reproduce the STAGS results presented here.

5. **Designers are urged to use the most generous fillet radii at intersections of panel skin and stringer web root that they can get away with**. STAGS or other general-purpose computer programs should be used to set up elaborate models in which the immediate neighborhood of the web root of at least one stringer is modeled with solid finite element in order to capture accurately what goes on in this critical regions in the post-local buckling loading regime.

Section 5.0
REFERENCES

[1] Bushnell, D., "PANDA2 - Program for minimum weight design of stiffened, composite, locally buckled panels", COMPUTERS AND STRUCTURES, Vol. 25, No. 4, pp 469-605, 1987

[2] Bushnell, D., "Theoretical basis of the PANDA computer program for preliminary design of stiffened panels under combined in-plane loads", COMPUTERS AND STRUCTURES, v. 27, No. 4, pp 541-563 (1987).

[3] Bushnell, D., "Optimization of composite, stiffened, imperfect panels under combined loads for service in the postbuckling   regime", Computer Methods in Applied Mechanics and Engineering, Vol. 103 (1993) 43-114

[4] Bushnell, D. and Bushnell, W. D., "Approximate method for the optimum design of ring and stringer stiffened cylindrical panels and shells with local, inter-ring, and general buckling modal imperfections" Computers and Structures, Vol. 59, No. 3, pp 489-527 (1996)

[5] Bushnell, D., "Recent enhancements to PANDA2" AIAA Paper 96-1337-CP, Proceedings of the AIAA 37th Structures, Structural Dynamics and Materials Conference, pp 126-182, April, 1996.

[6] Bushnell, D., Jiang, H., and Knight, N.F., "Additional buckling solutions in PANDA2", Proceedings of the 40th AIAA SDM Conference, AIAA Paper 99-1233, pp 302-345, April 1999

[7] Bushnell, D. and Rankin, C.C., "Optimization of perfect and imperfect ring and stringer stiffened cylindrical shells with PANDA2 and evaluation the optimum designs with STAGS", AIAA Paper 2002-1408, Proceedings of the AIAA 43rd SDM Meeting, pp 1562-1613, April 2002

[8] Bushnell, D. and Bushnell, W.D., "Minimum-weight design of a stiffened panel via PANDA2 and

evaluation of the optimized panel via STAGS", Computers and Structures, Vol. 50, No. 4, pp 569-602 (1994)

[9] Bushnell, D. and Bushnell, W.D., "Optimum design of composite stiffened panels under combined loading", Computers and Structures,Vol. 55, pp 819-856 (1995)

[10] Bushnell, D., "Optimum design via PANDA2 of composite sandwich panels with honeycomb or foam cores", AIAA Paper 97-1142, Proceeding of the 38th AIAA Structures, Structural Dynamics and Materials Conference, pp 2163-2202, April, 1997

[11] Bushnell, D., Rankin, C.C., and Riks, E., "Optimization of stiffened panels in which mode jumping is accounted for", AIAA Paper 97-1141, Proceedings of the 38th AIAA SDM Conference, pp 2123-2162, April 1997

[12] Bushnell, D., "Global optimum design of externally pressurized isogrid   stiffened cylindrical shells with added T-rings", Int. J. Non-Linear Mechanics, Vol. 37, Nos 4-5, pp 801-831 (2002)

[13] Bushnell, D., "Optimization of panels with riveted Z-shaped stiffeners via   PANDA2", in Advances in the Mechanics of Plates and Shells, Durban, D, Givoli, D., and Simmonds, J.G., Editors, Kluwer Academic Publishers, pp 79-102 (2001)

[14] Bushnell, D., "Truss-core sandwich design via PANDA2", Computers and Structures, Vol. 44, No. 5, pp 1091-1119 (1992)

[15] Bushnell, D., Holmes, A.M.C., Flaggs, D.L., McCormick,   P.J., "Optimum design, fabrication and test of graphite-epoxy curved, stiffened, locally buckled panels loaded in axial compression", in BUCKLING OF STRUCTURES, edited by I. Elishakoff, et al, Elsevier, Amsterdam, pp 61-131, 1988

[16] Bushnell, D. and Rankin, C.C., "Optimum design of stiffened panels with substiffeners", AIAA Paper 1932, 46th AIAA Structures, Structural Dynamics and Materials Meeting, Austin, TX, April 2005

[17] Bushnell, D. and Rankin, C.C., "Difficulties in optimization of imperfect stiffened cylindrical shells", AIAA Paper 1943, 47th AIAA Structures, Structural Dynamics and Materials Meeting, Newport RI, April 2006

[18] Bushnell, D. "Optimization of an axially compressed ring and stringer stiffened cylindrical shell with a general buckling modal imperfection", AIAA Paper 2007-2216, 48th AIAA SDM Meeting, Honolulu, Hawaii, April 2007

[19] Bushnell, D., .../panda2/doc/panda2.news, a continually updated file distributed with PANDA2 that contains a log of all significant modifications to PANDA2 from 1987 on.

[20] Vanderplaats, G. N., "ADS--a FORTRAN program for automated design synthesis, Version 2.01", Engineering Design Optimization, Inc, Santa Barbara, CA, January, 1987

[21] Vanderplaats, G. N. and Sugimoto, H., "A general-purpose optimization program for engineering design", Computers and Structures, Vol. 24, pp 13-21, 1986

[22] Koiter, W. T., "Het Schuifplooiveld by Grote Overshrijdingen van de Knikspanning", National Luchtvaart Laboratorium, The Netherlands, Report X295, November 1946 (in Dutch)

[23] B. O. Almroth, F. A. Brogan, "The STAGS Computer Code", NASA CR-2950, NASA Langley Research Center, Hampton, Va.(1978)

[24] C. C. Rankin, P. Stehlin and F. A. Brogan, "Enhancements to the STAGS computer code", NASA CR 4000, NASA Langley Research Center, Hampton, Va, November 1986

[25] Riks, E., Rankin C. C., Brogan F. A., "On the solution of mode jumping phenomena in thin walled shell structures", First ASCE/ASM/SES Mechanics Conference, Charlottesville, VA, June 6-9, 1993, in: Computer Methods in Applied Mechanics and Engineering, Vol.136, 1996.

[26] G. A. Thurston, F. A. Brogan and P. Stehlin, "Postbuckling analysis using a general purpose code", AIAA Journal, 24, (6) (1986) pp. 1013-1020.

APPENDIX

The figures, a1 – a5 are either cited or both cited and discussed in the text above.